



KADIR HAS UNIVERSITY  
SCHOOL OF GRADUATE STUDIES  
PROGRAM OF COMPUTATIONAL BIOLOGY AND BIOINFORMATICS

**DESIGN OF NOVEL AND POTENT INHIBITORS FOR mPGES-1  
ENZYME VIA IN SILICO SCREENING**

GAMZE ÇİFTÇİ

MASTER'S THESIS

İSTANBUL, July 2021

Gamze Çiftçi

MASTER'S THESIS

2021



**DESIGN OF NOVEL AND POTENT INHIBITORS FOR  
mPGES-1 ENZYME VIA IN SILICO SCREENING**

GAMZE ÇİFTÇİ

MASTER'S THESIS

Submitted to the School of Graduate Studies of Science and Engineering of Kadir Has University in partial fulfillment of the requirements for the degree of Master of Science in Program of Computational Biology and Bioinformatics

İSTANBUL, July 2021

DECLARATION OF RESEARCH ETHICS /  
METHODS OF DISSEMINATION

I, GAMZE ÇİFTÇİ, hereby declare that;

- this Master's thesis is my own original work, and that due references have been appropriately provided on all supporting literature and resources;
- this Master's thesis contains no material that has been submitted or accepted for a degree or diploma in any other educational institution;
- I have followed *Kadir Has University Academic Ethics Principles prepared in accordance with The Council of Higher Education's Ethical Conduct Principles*.

In addition, I understand that any false claim in respect of this work will result in disciplinary action in accordance with University regulations.

Furthermore, both printed and electronic copies of my work will be kept in Kadir Has Information Center under the following condition as indicated below

I do not want my thesis to be accessible for two years. If I do not apply for an extension at the end of this period, my thesis can be accessed in its entirety.

GAMZE ÇİFTÇİ  
TARİH VE İMZA

KADIR HAS UNIVERSITY  
SCHOOL OF GRADUATE STUDIES

**ACCEPTANCE AND APPROVAL**

This work entitled **DESIGN OF NOVEL AND POTENT INHIBITORS FOR mPGES-1 ENZYME VIA IN SILICO SCREENING** prepared by **GAMZE ÇİFTÇİ** has been judged to be successful at the defense exam on 30.07.2021 and accepted by our jury as master thesis.

APPROVED BY:

Prof. Dr. Kemal YELEKÇİ (Advisor)

Kadir Has University

\_\_\_\_\_

Prof. Dr. Safiye ERDEM

Marmara University

\_\_\_\_\_

Dr. Şebnem EŞSİZ GÖKHAN

Kadir Has University

\_\_\_\_\_

I certify that above signatures belong to the faculty members named above.

\_\_\_\_\_  
(Unvanı, Adı ve Soyadı)

Dean of School of Graduate Studies

DATE OF APPROVAL: (Gün/Ay/Yıl)

## TABLE OF CONTENTS

ABSTRACT .....	i
ÖZET.....	ii
ACKNOWLEDGEMENTS.....	iii
DEDICATION.....	iv
LIST OF TABLES .....	v
LIST OF FIGURES .....	vi
LIST OF SYMBOLS/ABBREVIATIONS.....	vii
<b>1. INTRODUCTION.....</b>	<b>1</b>
1.1 Properties of Microsomal Prostaglandin E Synthase-1 (mPGES-1) .....	1
1.2 Mechanism of mPGES-1 Enzyme Inhibition.....	2
1.3 Structural Studies of mPGES-1 Inhibition .....	4
<b>2. METHODS AND PROCEDURES .....</b>	<b>5</b>
2.1 Introduction .....	5
2.2 Preparation of Enzyme and Ligands .....	6
2.3 Virtual Screening with AutoDock-Vina .....	9
2.4 Docking Based Virtual Screening with AutoDock .....	9
2.5 ADMET .....	11
2.6 Molecular Dynamic simulations with NAMD .....	12
<b>3. RESULTS AND DISCUSSION .....</b>	<b>13</b>
3.1 AutoDock-Vina Results .....	13
3.2 Docking Results .....	14
3.3 ADMET Results .....	30
3.4 Molecular Dynamic Simulation Results .....	35
3.4.1 Root mean square deviation (RMSD) .....	35
3.4.2 Root mean square fluctuation (RMSF) .....	37
3.4.3 Radius of gyration (Rg) .....	39
<b>4. CONCLUSION.....</b>	<b>42</b>
<b>REFERENCES .....</b>	<b>44</b>
<b>CURRICULUM VITAE.....</b>	<b>49</b>

# DESIGN OF NOVEL AND POTENT INHIBITORS FOR mPGES-1 ENZYME VIA IN SILICO SCREENING

## ABSTRACT

To prevent inflammation in the body, non-steroidal anti-inflammatory drugs act by suppressing PGE2 production as a result of non-selective inhibition of both COX-1 and COX-2 enzymes. As a result of the inhibition of COX-1 and COX-2, gastrointestinal poisoning and cardiovascular complications occurred, respectively. mPGES-1 inhibitors have been shown to have no known side effects. Thus, inhibition of PGE2 biosynthesis by inhibition of mPGES-1 has become a new therapeutic target in the treatment of inflammatory diseases, which is considered to be clinically safer.

In this thesis, approximately 2.5 million ligands were downloaded from the ZINC particle library to screen the mPGES-1 enzyme. Prescreening of these ligands was performed with Autodock-Vina. 1261 compounds were scanned using Autodock 4. Binding energies and poses were determined. The best inhibitors were subjected to the ADMET test, and molecular dynamic simulation was performed for the four inhibitors determined as the best according to this test, and RMSD, RMSF, and Rg values were analyzed.

**Keywords:** mPGES-1 inhibitor, structure-based drug design, molecular modeling, NAMD

# SİLİKO TARAMA YOLUYLA mPGES-1 ENZİMİ İÇİN YENİ VE GÜÇLÜ İNİHİTÖRLERİN TASARIMI

## ÖZET

Vücutta oluşan enflamasyonu engellemek için steroid olmayan antienflamatuar ilaçlar her iki COX-1 ve COX-2 enzimlerinin seçici olmayan inhibisyonunun bir sonucu olarak PGE2 üretimini baskılayarak etki eder. COX-1 ve COX-2 'nin inhibisyonu sonucu sırasıyla gastrointestinal zehirlenmeler ve kardiyovasküler komplikasyonlar ortaya çıkmıştır. mPGES-1 inhibitörlerinin bilinen yan etkileri taşımadığı gösterilmiştir. Böylece, mPGES-1 inhibisyonu ile PGE2 biyosentezinin engellenmesi enflamatuvar hastalıkların tedavisinde, klinik olarak daha güvenli olduğu düşünülen, yeni bir terapötik hedef haline gelmiştir.

Bu çalışmada mPGES-1 enzimini taramak üzere ZINC parçacık kütüphanesinden yaklaşık 2.5 Milyon ligand indirilmiştir. Bu ligandların ön taramaları Autodock-Vina ile gerçekleştirilmiştir. 1261 bileşikte ise Autodock 4 kullanılarak tarama gerçekleştirilmiştir. Bağlanma enerjileri ve pozları belirlenmiştir. En iyi çıkan inhibitörler ADMET testine tabi tutulmuş ve bu testte göre de en iyi olarak belirlenen dört inhibitör için moleküler dinamik simülasyon gerçekleştirilerek RMSD, RMSF ve Rg değerleri analiz edilmiştir.

**Anahtar Sözcükler:** mPGES-1 inhibitörü, yapı odaklı ilaç tasarımı, moleküler modelleme, NAMD



## **ACKNOWLEDGEMENTS**

I am greatly thankful to my advisor, Prof. Dr. Kemal YELEKÇİ, for helpful discussions, guidance, and support. He always encouraged me in this process. Besides my advisor, I would like to thank the rest of my thesis committee.

I am really thankful to my friends for their whose encouragement and support helped me a lot during my Master's. Especially I thank my colleague Ammar Elmezayen for his support.

Last but not least, I would like to express my gratitude to my parents for their endless support and understanding no matter what.

Dedicated to My Parents ...

## LIST OF TABLES

Tablo 2.1	mPGES-1 crystal structures available in the RCSB protein database.....	7
Tablo 3.1	Binding energy values of the best 20 compounds according to Autodock-Vina for mPGES-1 .....	13
Tablo 3.2	Binding energy values of the best 20 compounds according to Autodock4 for mPGES-1 .....	14
Tablo 3.3	Types of interactions of the best ten inhibitors with the binding site residues of mPGES-1 enzyme.....	15
Tablo 3.4	Solubility and molecular descriptors of best ten compounds from SwissADME.....	31
Tablo 3.5	Predicted ADMET properties and drug-likeness of best ten compounds .....	33

## LIST OF FIGURES

Figure 1.1	mPGES-1 pathways .....	3
Figure 2.1	Graphical abstract for identification of potential mPGES-1 inhibitors.....	5
Figure 3.1	3D and 2D image of compound 6PW .....	16
Figure 3.2	3D and 2D image of I197821 compound.....	17
Figure 3.3	3D and 2D image of H453361 compound .....	18
Figure 3.4	3D and 2D image of J193055 compound.....	19
Figure 3.5	3D and 2D image of J193395 compound.....	20
Figure 3.6	3D and 2D image of H415814 compound .....	21
Figure 3.7	3D and 2D image of H455638 compound .....	22
Figure 3.8	3D and 2D image of I198359 compound.....	23
Figure 3.9	3D and 2D image of I318035 compound.....	24
Figure 3.10	3D and 2D image of I318035 compound .....	25
Figure 3.11	3D and 2D image of J193203 compound .....	26
Figure 3.12	2D Molecule structures of highly selective ligands.....	27
Figure 3.13	The predictive model of BOILED-Egg for the best ten drug precursor molecules.....	34
Figure 3.14	50 ns-MD simulation RMSD profiles of free mPGES-1 and bound mPGES-1 enzyme .....	36
Figure 3.15	RMSF profiles of the free mPGES-1 and bound mPGES-1 enzyme .....	38
Figure 3.16	Rg profiles of the free mPGES-1 and bound mPGES-1 enzyme .....	40

## LIST OF SYMBOLS/ABBREVIATIONS

Å	Angstrom
K	Kelvin
%	Percentage
$\pi$	Pi
3D	Three Dimensional
2D	Two Dimensional
mPGES-1	Microsomal Prostaglandin E Synthase-1
PGs	Prostaglandins
PGE2	Prostaglandin E2
AA	Arachidonic Acid
COX-1	Cytochrome c oxidase subunit I
COX-2	Cytochrome c oxidase subunit II
PGH2	Prostaglandin H2
GSH	Glutathione
PDB	Protein Data Bank
NAMD	Nanoscale Molecular Dynamics
VMD	Visual Molecular Dynamics
Pdbqt	Protein Data Bank, Partial Charge (Q), & Atom Type (T)
OPM	Orientations of Proteins in Membranes
POPC	1,2-palmitoyl-oleoyl-sec glycerol-3-phosphocholine
MD	Molecular Dynamics
NaCl	Sodium Chloride
ns	Nanosecond
LGA	Lamarckian Genetic Algorithm
RMSD	Root Mean Square Deviation
RMSF	Root Mean Square Fluctuation
Rg	Radius of gyration

MW	Molecular Weight
LogP	Lipophilicity
LogS	Water Solubility
HBA	Hydrogen Bond Acceptor
HBD	Hydrogen Bond Donor
nRot	Rotatable Bond Number
TPSA	Topological Polar Surface Area
P-gp	P-glycoprotein
ATP	Adenosine Triphosphate
BBB	Blood-Brain Barrier
CNS	Central Nervous System
SER	Serine
THR	Threonine
HIS	Histidine
ARG	Arginine
ASN	Asparagine
GLU	Glutamate
TYR	Tyrosine

# 1. INTRODUCTION

## 1.1 Properties of Microsomal Prostaglandin E Synthase-1 (mPGES-1)

Prostaglandins (PGs), a critical bioactive derivative of arachidonic acid, have essential roles in physiological events such as homeostasis, fever, gastrointestinal motility, pain, and inflammation in the human body (Murakami, 2011). PGs also play an essential role in angiogenesis. In particular, PGE2 is a crucial PG in stimulating angiogenic behavior (Norel, 2007). In addition, recent studies have shown that the stromal PGE2-EP3 receptor is required for tumor growth and angiogenesis (Amano et al., 2003).

During inflammation, mPGES-1 is responsible for the pathogenic amount of production of inflammatory PGE2, a member of the PG family (Akasaka et al., 2015). It has been reported that mPGES-1 enzyme is associated with many types of cancer such as colon (Sasaki et al., 2015), lung (Chang & Meuillet, 2011), breast (Howe et al., 2013), prostate (Hanaka et al., 2009), gastric adenocarcinoma (Van Rees et al., 2003), and neuroblastoma (Kock et al., 2018). This shows that PGES-1 is a multiple target for many cancer types.

mPGES-1 is also known to be associated with the induction of tumor progression (Jakobsson et al., 1999). Genetic deletion of mPGES-1 reduces proliferation and angiogenesis (Finetti et al., 2012). In addition, studies revealed decreased tumor-induced angiogenesis and inhibition of chronic inflammation in mice lacking mPGES-1 (Kamata et al., 2010).

## 1.2 Mechanism of mPGES-1 Enzyme Inhibition

PGE2 biosynthesis is dependent on the release of arachidonic acid (AA) from phospholipids in the cell membrane via the phospholipase A2 enzyme. The released AA is then converted to PGH2 by the enzymes cyclooxygenase COX-1 and COX-2. PGH2 is converted to PGE2 via three different PGE2 synthases, microsomal PGE2 synthase-1 and -2 (mPGES-1 and -2) and cytosolic PGE2 synthase (cPGES), as shown in **Figure 1.1**. In addition to PGE2, PGH2 also acts as a central precursor substrate for many physiologically important PG and TXB2 biosynthesis via different PG synthases and thromboxane (Tx) synthase (Chang & Meuillet, 2011) .

Non-steroidal anti-inflammatory drugs (NSAIDs) available in clinical use act by suppressing PGE2 production due to non-selective inhibition of COX-1 and COX-2 enzymes. Of these, COX-1 enzyme directs the biosynthesis of PGs involved in maintaining the regular activity and homeostasis of specific cells. At the same time, COX-2 has been identified as the inducible isoform responsible for inflammatory PGE2 biosynthesis (Luz et al., 2015).

Since COX enzymes catalyze the first step of Tx and PG synthesis, inhibition of COX enzyme in a cell with drugs affects all PG and Tx production, and these drugs cause severe gastrointestinal side effects if used for a long time. Furthermore, drugs developed later that selectively suppress inflammatory PGE2 formation as a result of their COX-2 inhibitory effects also caused serious cardiovascular complications since they also inhibited the formation of antithrombotic prostacyclin and were discontinued from treatment (Zhou et al., 2017).



For this reason, as the newest approach, it is aimed to develop new molecules that are safer for clinical use and do not contain the above side effects by preventing PGE2 formation from AA with mPGES-1 inhibitors, only inflammatory PGE2 formation in the last step of the pathway. Studies are ongoing to develop new mPGES-1 inhibitors. However, none of the new inhibitor candidates has reached clinical trials and phase I studies (Jin et al., 2018).

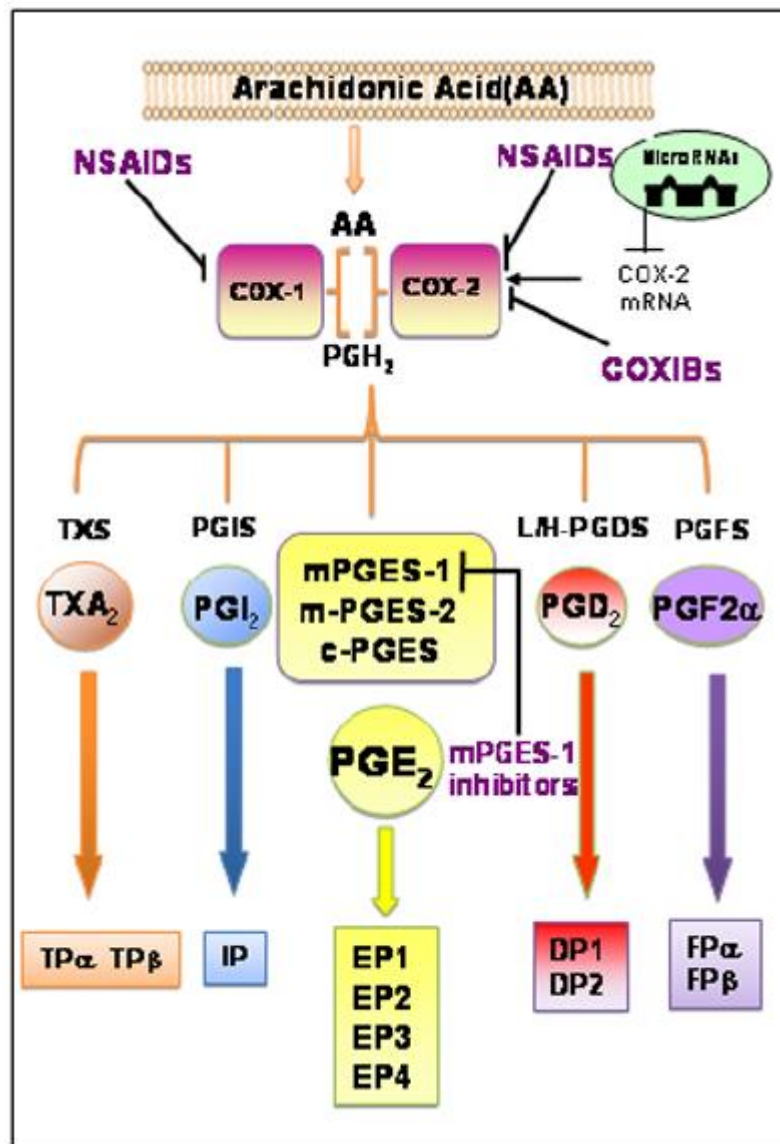


Figure 1.1: mPGES-1 pathway (D Isaacson, J L Mueller, 2006)

### **1.3 Structural Studies of mPGES-1 Inhibition**

mPGES-1 inhibitors were designed and molecularly modeled using some scaffolds for binding with human and mouse mPGES-1 enzymes. It was aimed that these inhibitors, which were intended, could bind appropriately to both human and mouse mPGES-1 enzymes. Using the new scaffold, a set of 10 novel compounds was tested against human and mouse mPGES-1 enzymes for their inhibitory activity in vitro (Ding et al., 2018).

A large database of lead compounds was first scanned virtually to retrieve putative mPGES-1 inhibitors. Essential amino acids involved in antagonist recognition were identified by known compound-based comparison. According to homology patterns, the binding pocket of the mPGES-1 receptor overlapped with both the binding site of the PGH2 substrate and the GSH cofactor in the mPGES-1 protein. Due to the high affinity of known mPGES-1 inhibitors, there must be inhibitors that participate in some fundamental interactions and move away from the active site (Hamza et al., 2011).

## 2. METHODS AND PROCEDURES

### 2.1 Introduction

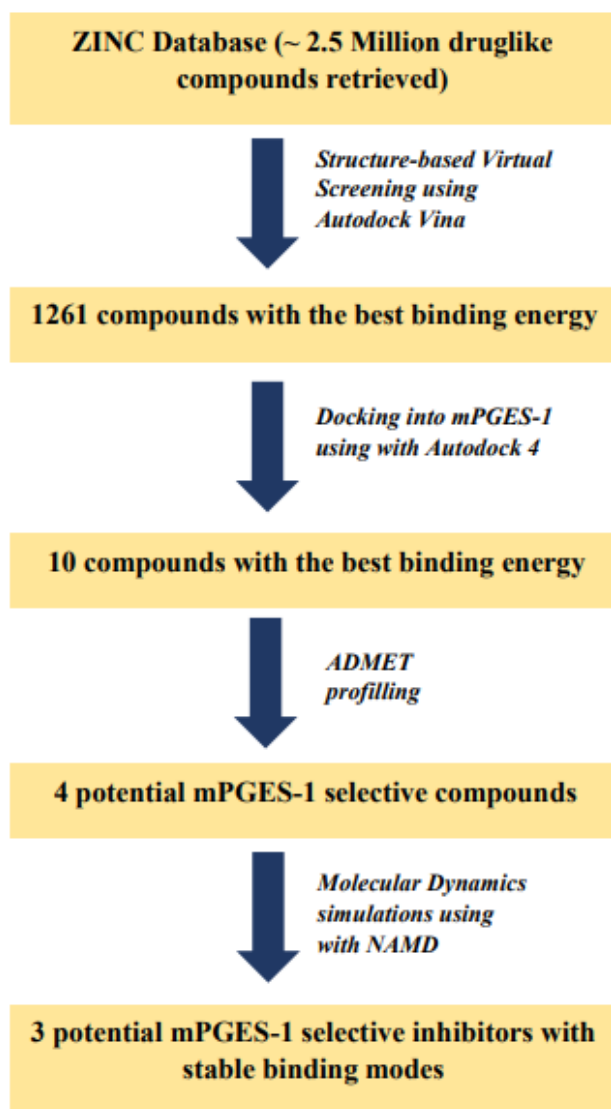


**Figure 2.1.** Graphical abstract for identification of potential mPGES-1 inhibitors.

were selected from 20 molecules with the best binding energy, and their binding energies, binding poses, and ADMET values were investigated in detail. As a result of these investigations, Molecular Dynamics studies were carried out using NAMD to support the inhibition of 4 potential mPGES-1 potent compounds in static binding mode. According

The methods used in the study while finding potential selective inhibitors against the mPGES-1 enzyme are shown in *Figure 2.1* as a graphical summary. Approximately 2.5 million drug-like compounds were downloaded from the ZINC library to screen for inhibition against the mPGES-1 enzyme. All these downloaded compounds were in sdf format. In order to filter these ligands, Autodock-Vina, which is the preferred fast and reliable structure-based screening method, was selected. All ligands in pdb format were converted to pdbqt format when using Autodock-Vina. According to the Autodock-Vina results, the first 1261 drug-like molecules with the best binding energy were screened using Autodock 4. According to Autodock 4 results, ten molecules

to simulation analyzes performed using Visual Molecular Dynamics (VMD) software, two potential mPGES-1 potent inhibitors were detected in fixed binding mode.

## 2.2 Preparation of Enzyme and Ligands

For the crystal structure to be used for the target protein in the docking study, our relevant protein crystal structures were examined according to the order of the article published recently from Protein Data Bank (<https://www.rcsb.org/>). Two forms drew attention in this review. When deciding which of these structures to use, the primary part that was looked at was the resolution of the crystal structures. Data quality is a measure that is resolution, collected on crystals containing protein or nucleic acids. If all the proteins in the crystal are aligned the same, forming a perfect crystal, then all the proteins scatter X-rays in the same way, and the diffraction pattern shows the fine details of the crystal.

On the other hand, if the proteins in the crystal are all slightly different due to local elasticity or movement, the diffraction pattern will not contain much delicate information. The resolution, then, measures the level of detail found in the diffraction pattern and the level of detail that can be seen when the electron density map is calculated. High-resolution structures with resolution values of 1 Å or more are highly ordered, and each atom is easy to see on the electron density map. Lower resolution structures with a resolution of 3 Å or higher show only the basic contours of the protein chain, and the atomic structure must be removed. Therefore, the choice is always a high-resolution structure. Thus, while choosing the crystal structure, care was taken to ensure that the resolution is lower than 2 Å, that is, high resolution (Foley, 1991). Although there are nine mPGES crystal structures, shown in **Table 2.1**, validation studies have been carried out with mPGES inhibitors with the best resolution in the protein database. The experimental values of the structure have been used in the minimized crystal structure modeling studies. After investigations, it was decided to work with 5K0I crystal structure.

			<i>Experimental Data Snapshot</i>				
<i>PDB</i>					<i>R-Value</i>	<i>R-Value</i>	<i>R-Value</i>
<i>Kodu</i>	<i>Mutation</i>	<i>Organism</i>	<i>Method</i>	<i>Resolution</i>	<i>Free</i>	<i>Work</i>	<i>Observed</i>
5K0I	Hayır	Homo sapiens	X-Ray Diffraction	1.30 Å	0.159	0.145	0.146
5TL9	Hayır	Homo sapiens	X-Ray Diffraction	1.20 Å	0.168	0.152	0.153
4YL1	Hayır	Homo sapiens	X-Ray Diffraction	1.41 Å	0.175	0.163	0.163
4YL0	Hayır	Homo sapiens	X-Ray Diffraction	1.52 Å	0.220	0.196	0.198
4AL0	Hayır	Homo sapiens	X-Ray Diffraction	1.16 Å	0.130	0.122	0.122
5BQG	Hayır	Homo sapiens	X-Ray Diffraction	1.44 Å	0.169	0.150	0.151
5T37	Hayır	Homo sapiens	X-Ray Diffraction	1.76 Å	0.185	0.167	0.168
5T36	Hayır	Homo sapiens	X-Ray Diffraction	1.40 Å	0.195	0.184	0.184
4BPM	Evet	Homo sapiens	X-Ray Diffraction	2.08 Å	0.218	0.200	0.201

**Table 2.1** mPGES-1 crystal structures available in the RCSB protein database

The "PDB" format of the 5K0I (PDB ID: 5K0I, resolution: 1.30 Å) (Kuklish et al., 2016) crystal structure downloaded from the Protein Data Bank (<https://www.rcsb.org>), an online database of proteins, which is one of the selected structures, was opened in Biovia Discovery Studio 4.5 (DS) (Dassault Systemes BIOVIA, 2017). Other molecules (water, ligands, etc.) in the protein were cleaned in this opened form. The region where the 6PW ligand is bound was accepted as the active site, showing the best binding with the protein (determined by looking at **Table 2.1** in PDB) and the region's coordinates where this ligand is bound in the region protein was determined. These coordinates were used as active sites in docking studies. All missing hydrogens were added, and Biovia DS 4.5 was used to optimize by selecting the "Clean Geometry" toolkit with a fast, Deriding-like forcefield.

Further, energy minimization of the protein was carried out utilizing the "Prepare Macromolecule" protocol of DS with the assignment of CHARMM force field based on the protonation state of the titratable residues at physiological pH 7.4.

Glutathione, the second ligand of the protein, was used throughout the docking studies. Because the structure of the mPGES-1 enzyme forms a homotrimer, only one monomer is active at a time in the open conformation of the enzyme used for modeling studies. mPGES-1 catalyzes the isomerization of PGH2 to PGE2, and glutathione (GSH) is an essential cofactor for its catalytic turnover. GSH is bound within the active site in a U-shaped conformation via hydrogen bonds (Arg 38, Arg73, Asn74, Glu77, His113, Tyr117, Arg126, and Ser127), pi-pi stacking (Tyr130) interactions as well as other hydrophobic and polar interactions. The experimental results indicated that a potential inhibitor could act as a false substrate (PGH2) and a cofactor analog (GSH) in a structure-based design. Thus, the U-shape conformation of ligands inactive site is essential for inhibition of this enzyme. Most known mPGES-1 inhibitors bind to the substrate and glutathione (GSH) cofactor binding sites simultaneously (Serhan et al., 2019). Therefore, the substrate and cofactor binding pockets volume were utilized for the docking studies. Energy minimization was carried out. The protein was recorded in this state in pdb format. The protein opened in pdb format in AutoDock 4.2.6 docking program was converted to pdbqt format in this program. Ligands downloaded from the ZINC library. This database is available for free download (<http://zinc.docking.org>) in several common file formats, including SMILES, mol2, 3D SDF, and DOCK flexible format. A Web-based query tool incorporating a molecular drawing interface enables the database to be searched and browsed and subsets to be created. Users can process their own molecules by uploading them to a server (Irwin & Shoichet, 2005). Ligands were downloaded in sdf format and first converted in pdb format using the openbabel program (Melville & Hirst, 2007). The ligands converted to pdb format were converted to pdbqt format using the same program. The purpose of converting from pdb format to pdbqt format is to assign partial charges of each atom using Gastiege-Marcilli method (Ref). Ligand files are converted to pdbqt format were primarily used in the AutoDock-Vina program in the first screening phase. After AutoDock-Vina, ligands and enzyme structures were used as input files for grid mapping and docking.

### 2.3 Virtual Screening with AutoDock-Vina

Structure-based virtual screening is a widely used method in academic laboratories to determine the chemical structures of novel drug candidates (Patrick Walters et al., 1998). Using a hybrid scoring system (experimental + knowledge-based), Autodock Vina is faster than other building-based virtual programs. For this reason, it is an ideal program to screen a large number of drug precursor molecules. Autodock-Vina automatically calculates grid maps and transparently presents the results to the user (Allouche, 2012) (<http://vina.scripps.edu>). Also, the time spent on the search varies depending on the number of atoms and flexibility. As a first step, Autodock-Vina was used to screen about 2.5 Million drug-like compounds from the ZINC library against the enzyme mPGES-1 (PDB ID: 5K0I, resolution: 1.30 Å) (Kuklish et al., 2016). Grid center sizes 60, 60, 60 Å, and the grid box center was determined as 9.697 x 15.296 x 27.28 (x y z). First, the compounds downloaded from the ZINC library and scanned with Autodock-Vina were filtered according to their binding energy values. 1261 drug precursor was selected for use in Autodock 4.2.6 for the orientation of ligands at the molecule binding site.

### 2.4 Docking Based Virtual Screening with AutoDock

Screened with Autodock-Vina and filtered according to binding energy values, 1261 drug precursor molecules were selected in Autodock 4.2.6, one of the structure-based virtual screening methods, for further investigation. AutoDock 4.2.6 nesting program (<http://autodock.scripps.edu>) was used for all nesting experiments (Allouche, 2012). All ligands were set to be flexible, but the protein was set to be rigid. The region where the 6PW ligand occupied a volume during crystallization was considered the enzyme's active site. Before virtual scanning, validation studies started to prepare the gpf file. For the active region of the crystal structure determined in the Gpf file, the dimensions were defined as 60 x 60 x 60 Å together with the coordinates of 9.697 x 15.296 x 27.28 (x y z); these measurements included the size of the prepared compounds. While preparing the dpf file, the parameters were determined as follows.

Lamarckian Genetic Algorithm (Morris et al., 1998) of Autodock 4.2 with 20,000,000 energy evaluations was used for ligand conformational search. Lamarckian Genetic Algorithm was chosen because the genetic algorithm only performs a general search, but the Lamarckian Genetic Algorithm is a hybrid algorithm (both genetic and local search). Hence, it is more efficient and has improved performance based solely on the genetic algorithm. In the Lamarckian Genetic Algorithm, a local search is done after each generation at a user-defined population ratio. However, many factors affect the quality of the results we can obtain using the Genetic Algorithm and Lamarckian Genetic Algorithm. First, it starts with a population of random ligand forms of both the Genetic Algorithm and the Lamarckian Genetic Algorithm in random orientations and random translations (Allouche, 2012). Then, the number of individuals in the population is decided using "ga\_pop\_size." AutoDock counts the number of energy assessments and the number of generations as the docking work progresses: the run ends when any of the limits are reached ("ga\_num\_evals" and "ga\_num\_generations," respectively). Using "ga\_elitism" the number of best individuals surviving in the next generation was automatically determined in the current population; typically, this is 1. Also, a value was specified for the gene mutation rate using "ga\_mutation\_rate" and for the gene transition rate "ga\_crossover\_rate." Typically, these are 0.02 and 0.80. To select the worst individual, the generation number is determined by "ga\_window\_size" and is usually 10. "Ga\_run" indicates the number of conformations. It was initially set to 20 runs, but this run count significantly slowed down the docking work. That's why ga\_run changed to 10. As a result of docking, not 20 conformations as at the beginning; Ten independent runs were performed for each ligand. The different conformers produced were randomly placed at the active site of these enzymes. The Biovia Discovery studio visualizer program was used to process interactions between ligand-protein complexes. In the docking study, the dpf file was prepared using the following parameters.

```
ga_pop_size 150           # number of individuals in population
ga_num_evals 2500000     # maximum number of energy evaluations
ga_num_generations 27000 # maximum number of generations
ga_elitism 1             # number of top individuals to survive to next generation
ga_mutation_rate 0.02   # rate of gene mutation
```



```
ga_crossover_rate 0.8      # rate of crossover
ga_window_size 10         #
ga_run 10                  # do this many hybrid GA-LS runs
```

1261 compounds scanned using all these parameters were first filtered for their binding energies. Secondly, attachment poses were examined. In the light of the 3D and 2D images taken, the binding poses of the first ten ligands with the best binding energy were observed as expected. Ten drug precursor molecules showing the best binding energy and binding exposure were evaluated to look at ADMET values.

## 2.5 ADMET

As a result of the modeling studies on the compounds downloaded from the ZINC library, ten molecules with the best binding energy and showing the best binding poses were selected with the mPGES-1 enzyme. ADMET studies were carried out in detail on ten chosen molecules. ADMET stands for Absorption, Distribution, Metabolism, Excretion, and Toxicity. The prediction of ADMET properties of the ten molecules that show the best inhibition is significant in the drug design process. ADMET properties are responsible for the clinical failure of the drug precursor molecules that have reached the clinical stage, such as the ligands used in this study, at a rate of 60% (Allouche, 2012). For a drug precursor molecule to be a drug, it must contain all ADMET properties.

ADMET profile showing Caco2 permeability and P-glycoprotein substrate (absorption) in this study; BBB and CNS permeability (distribution); CYP450 enzyme inhibition (metabolism); total clearance (excretion); AMES toxicity (toxicity) etc. The properties of mutagenic, tumorigenic, reproductive, and irritant effects and drug affinity of selected active compounds were examined. All these features were performed using online web server SwissADME (<http://www.swissadme.ch>) (Daina et al., 2017), online webserver admetSAR (<http://lmmd.ecust.edu.cn/admetSar2/>) (Cheng et al., 2012), online webserver pkCSM (<http://biosig.unimelb.edu.au/pkCSM>) (Pires et al., 2015) and OSIRIS Data warrior software (<http://www.openmolecules.org/datawarrior>) (Sander et al., 2015).

## 2.6. Molecular Dynamic simulations with NAMD

Among the nearly 2.5 million compounds screened only best four compounds were used for MD Simulation. It was performed for four compounds using NAMD (<http://www.ks.uiuc.edu/Research/namd/>) simulation program was utilized in this study (Phillips et al., 2005). Since mPGES-1 is a membrane-bound protein, it cannot be prepared directly with water molecules, and this protein must be fixed to the membrane. Thus, using the OPM web service (<http://opm.phar.umich.edu>) (Lomize et al., 2006), 1,2-palmitoyl-oleoyl-sec glycerol-3-phosphocholine (POPC) was added to the membrane prior to the preparation of the input files. CHARMM-GUI web service (<http://www.Charmm.org>) (Lee et al., 2016) was used for input parameter files to be used in NAMD MD simulation software. In this web service, the system was decoded using the TIP3P water model; the water molecules were protected and neutralized by adding 0.15 M NaCl to the ionic concentration. In the first minimization (1000 steps), the lipid tails were left mobile to induce the structure of the membrane, and the other parts (lipid head groups, ion, etc.) were kept constant. After the first minimization, the system was rebooted using Langevin dynamics at 303.15 K. The equilibrium of the system was achieved with a time step of 2 fs for 1 ns. In the second minimization (1000 steps), the protein backbone was limited by harmonic constraints. The system, in which water molecules were prevented from entering the hydrophobic zone of the membrane, was balanced for 1 ns. By releasing harmonic constraints in ultimate minimization, the system is further balanced. The production run was carried out without any restrictions for 50 ns at 303.15 K and 1 atm. To compare the stability of all 4 ligands with the protein by MD Simulation, the protein was run in a membrane system alone. Stability of ligand binding modes in the system, root mean square deviation (RMSD), root mean square fluctuation (RMSF), radius of gyration (Rg), and the energies of the systems were calculated and compared. All these investigations were done using Visual Molecular Dynamics (VMD) software (Yamada et al., 2017).

### 3. RESULTS AND DISCUSSION

#### 3.1 AutoDock-Vina Results

Compound Code	ZINC ID Code	Binding Energy (kcal/mol)
H196879	ZINC00001476141	-8.1
H233078	ZINC000012088315	-7.7
H285055	ZINC000006623685	-7.6
H288489	ZINC000006725168	-7.6
H308893	ZINC000012156772	-7.5
H321769	ZINC000002965628	-7.5
H415814	ZINC000002385836	-7.3
H416840	ZINC000039778397	-7.3
H419219	ZINC000012944048	-7.2
H440150	ZINC000072359656	-7.2
H448171	ZINC000000903003	-7.1
H453361	ZINC000009169466	-7.1
H455638	ZINC000012542713	-7.1
H455875	ZINC000003440203	-7
H456046	ZINC000004108162	-7
H456446	ZINC000226768390	-7
I197821	ZINC000008826383	-7
I198359	ZINC000009335330	-6.9
I210337	ZINC000095995831	-6.9
I218834	ZINC000012703899	-6.9

**Table 3.1** Binding energy values of the best 20 compounds according to Autodock-Vina for mPGES-1.

In total, approximately 2.5 Million ligands were retrieved via ZINC library. All ligands were simultaneously docked via AutoDock-Vina program. 1261 ligands were selected according to AutoDock-Vina result, which is positive for mPGES-1. The best 20 ligands in the selected ligands, according to AutoDock-Vina results, are shown in **Table 3.1**. Having a positive score of free energy for a ligand means that;  $K_i$  values could not be calculated since they are unfavorable for mPGES-1, and it is unusable. After obtaining results, the best mPGES-1 inhibitors were determined according to the total score of binding energy.

The compounds are among the ligands used to perform the next step, Autodock 4 studies. Since approximately 2.5 million ligands were screened at this stage, the binding energy was used as the selection parameter. Drug precursor molecules with binding energies greater than -5.00 were not used in AutoDock 4 studies. Therefore, 1261 pre-drug molecules with binding energies less than -5.00 were selected.

### 3.2 Docking Results

Compound Code	ZINC ID Code	Binding Energy (kcal/mol)
6PW		-5.22
I197821	ZINC000008826383	-9.42
H453361	ZINC000009169466	-9.26
J193055	ZINC000009402864	-9.26
J193395	ZINC000021416237	-9.19
H415814	ZINC000002385836	-9.18
H455638	ZINC000012542713	-9.04
I198359	ZINC000009335330	-8.97
I318035	ZINC000009190308	-8.96
J208987	ZINC000035485287	-8.96
J193203	ZINC000009441172	-8.86
I282820	ZINC000053224602	-8.80
H440150	ZINC000072359656	-8.77
H285055	ZINC000006623685	-8.75
J211739	ZINC000101359119	-8.75
H456046	ZINC000004108162	-8.70
J193468	ZINC000013141538	-8.68
I319486	ZINC000219162141	-8.66
J192648	ZINC000009964020	-8.64
I311871	ZINC000257198481	-8.63
J214049	ZINC000002126228	-8.63

**Table 3.2** Binding energy values of the best 20 compounds according to Autodock4 for mPGES-1.

The computational binding energies of compounds docked with the mPGES-1 enzyme are shown in **Table 3.2**. 6PW with the best experimental inhibition value was used as a control in a concurrent insertion to discuss the program's validity and find a better and highly potent mPGES-1 inhibitor than currently commercially available inhibitors (Kuklish et al., 2016). Of the 1261 compounds used in the AutoDock 4 study, compounds I197821, H453361, J193055, and J193355 with the best binding energies among the 20 molecules that provided the best inhibition showed better binding energies than the reference compound 6PW. The insertion poses of ten compounds with good binding energies and inhibition and

compound 6PW are detailed to see their interactions with residues covering the enzyme's active site (**Table 3.3**). As a result of molecular docking studies, it was found that the most active compounds I197821, H453361, J193055, and J193355 have a U-shaped conformation in the active site. Furthermore, strong hydrogen bonding with Arg126 was observed and a pi-pi stacking interaction with a Tyr130, especially with active site residues supporting better binding energies than other compounds, which is almost common to all compounds.

Compound Code	ZINC ID Code	Number of H-bonds	Distance of H-bonds (Å)	H-bonds interactions	Hydrophobic interactions
6PW		2	2.23 3.11	ARG126 : H (O-H) ASN74 : O	TYR130 (pi alkly)(3) ALA130 (pi alkly)
I197821	ZINC000008826383	2	2.81 2.66	ARG126 : O (C=O) TYR117 : O	TYR130 (pi-pi stacking)(3)
H453361	ZINC000009169466	2	2.21 3.12 2.93	THR131 : H (N-H) THR131 : O (C=O) ARG126 : O (C=O)	TYR130 (pi-pi stacking)(2) ARG126 (pi-cation)(2)
J193055	ZINC000009402864	5	2.68 3.35 1.90 2.06	ARG126 : O TYR117 : O (C=O) SER127 : H (N-H) THR131 : H (N-H)	TYR130 (pi-pi stacking)(3)
J193395	ZINC000021416237	4	2.61 1.80 2.53 3.12	THR131 : H (N-H) THR131 : O SER127 : H (N-H) ARG126 : O (C=O)	TYR130 (pi-pi stacking)(3) THR131 (pi-sigma)
H415814	ZINC000002385836	3	3.35 3.12 3.10	ARG126 : O (C=O) TYR117 : O (C=O) ARG73 : O (C=O)	TYR130 (pi-pi stacking)(2) ARG126 (pi-cation)(2) ARG70 (pi-cation) ARG73 (pi-cation)
H455638	ZINC000012542713	2	2.34 2.73	GLU77 : H(N-H) ARG126 : O (C=O)	TYR130 (pi-pi stacking) ARG73 (pi-cation)
I198359	ZINC000009335330	4	2.75 2.70 3.08 2.13	ARG126 : O (C=O) ARG73 : O (C=O) TYR117 : O HIS113 : H (N-H)	TYR130 (pi-pi stacking)(3)
I318035	ZINC000009190308	2	2.60 3.33	ARG126 : O THR131 : S	TYR130 (pi-pi stacking)(2) TYR130 (pi-sulfur)
J208987	ZINC000035485287	2	2.24 3.20	TYR130 : H (N-H) ASN74 : O (C=O)	TYR130 (pi-pi stacking)(2) ARG126 (pi-cation) GLU77 (pi-cation)(2)
J193203	ZINC000009441172	5	3.11 3.08 2.83 3.25 2.70	ARG126 : O (C=O) SER127 : O (C=O) ASN74 : O (C=O) ASN74 : O (C=O) ARG73 : O (C=O)	TYR130 (pi-pi stacking) ARG126 (pi-cation)

**Table 3.3** Types of interactions of the best ten inhibitors with the binding site residues of mPGES-1 enzyme.

2D and 3D images of the interaction of reference compound 6PW with the mPGES-1 enzyme are given in **Figure 3.1** for comparison with other ligands.

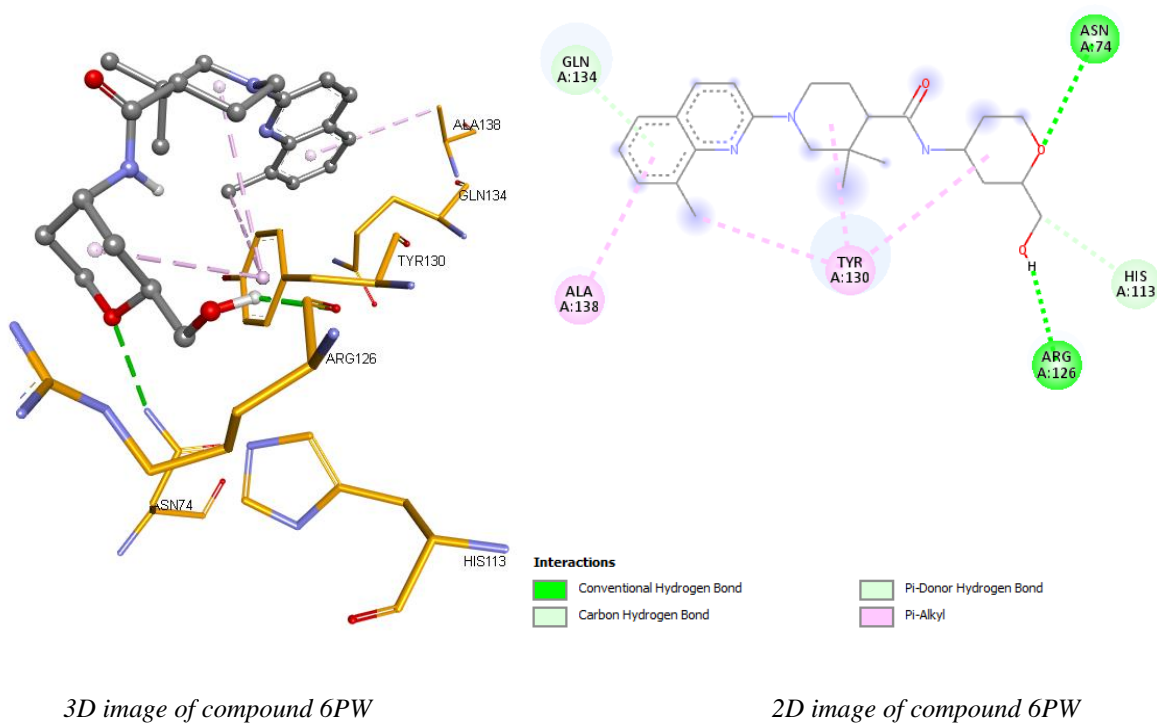
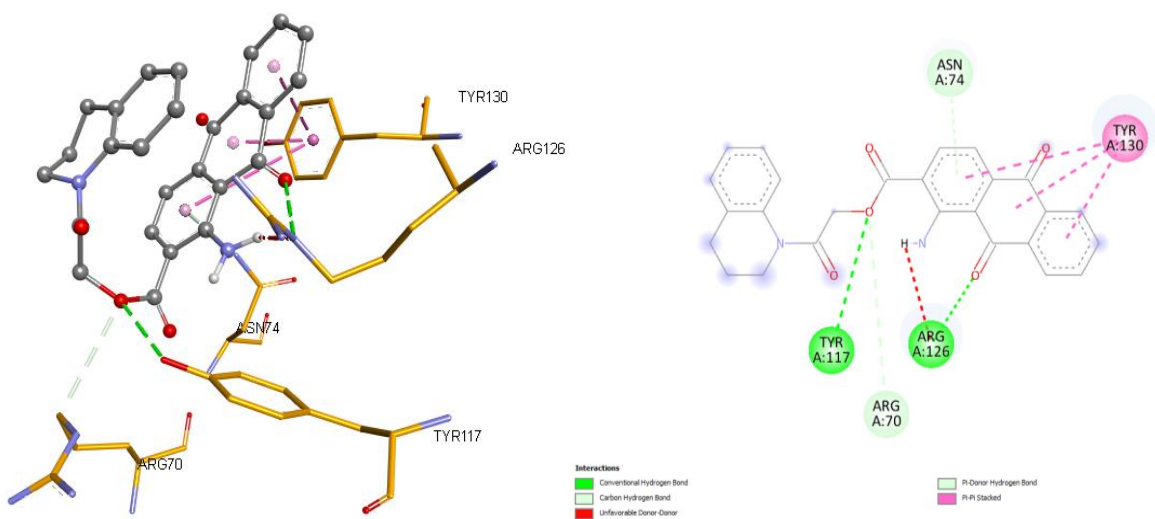


**Figure 3.1** 3D and 2D image of compound 6PW

2D and 3D images of the interaction of the I197821, with the mPGES-1 enzyme are given in **Figure 3.2** for comparison with others. Pi-pi stacking hydrophobic interaction was observed with Tyr130 and strong hydrogen bonds with Arg126, which was seen similarly in the 6PW compound in I197821 compound. In addition to the reference compound 6PW, it was observed that compound I197821 made strong hydrogen bond with Tyr117. The effect of these strong hydrogen bond on strong bonding was also reflected positively.



*3D image of compound I197821*

*2D image of compound I197821*

**Figure 3.2** 3D and 2D image of I197821 compound

2D and 3D images of the interaction of the H453361 with the mPGES-1 enzyme are given in **Figure 3.3** for comparison with others. In the H453361 compound, pi-pi stacking hydrophobic interaction was observed with Tyr130, which was seen similarly in the 6PW compound. Pi-cation hydrophobic interaction with Arg126, which was not observed in 6PW, was also observed. In addition to the reference compound 6PW, it was observed that H453361 made strong hydrogen bonds with Thr131. The effect of these strong hydrogen bonds and hydrophobic interactions on strong bonding was also reflected positively.

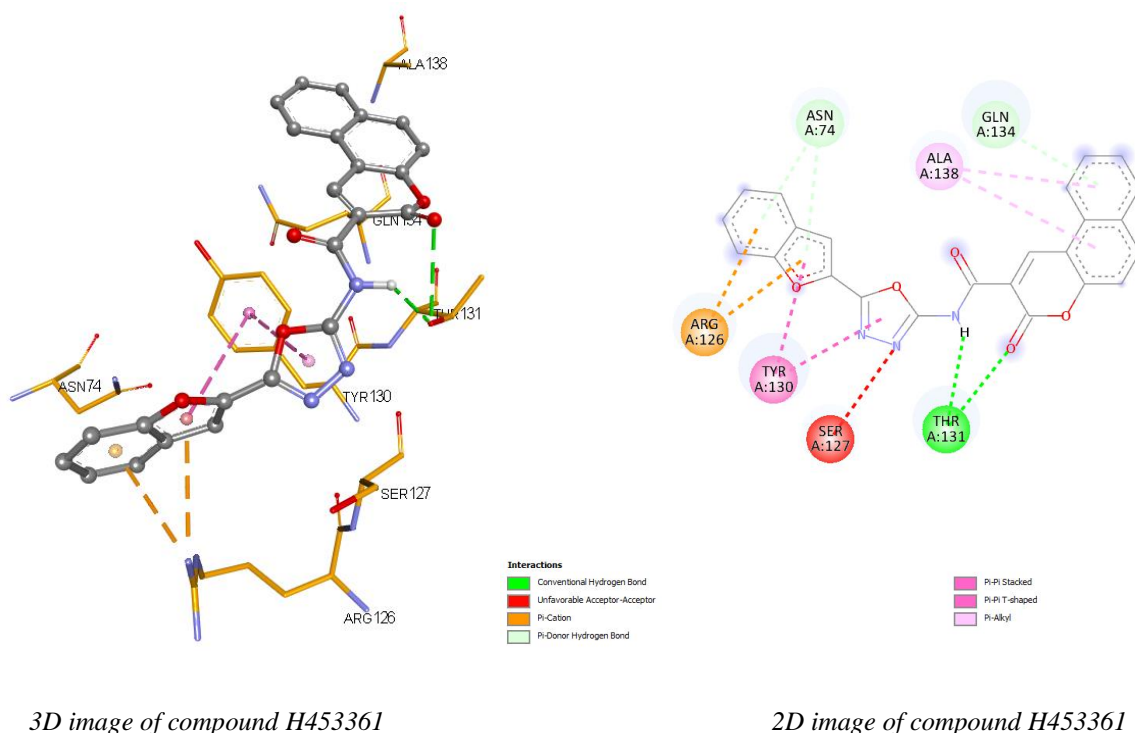


**Figure 3.3** 3D and 2D image of H453361 compound



2D and 3D images of the interaction of the J193055 with the mPGES-1 enzyme are given in **Figure 3.4** for comparison with other. Pi-pi stacking hydrophobic interaction was observed with Tyr130, which was seen similarly in 6PW compound in J193055 compound. There were strong hydrogen bonds observed in compound J193055 in addition to the reference compound 6PW. These are strong hydrogen bonds interacting with Tyr117, Ser127, and Thr131. The effect of these strong hydrogen bonds on strong bonding was also reflected positively. Strong hydrogen bond interactions observed with Arg126 and Tyr 117 were also observed in compound I197821. These two hydrogen bonds have a high effect on strong bonding. In addition, the strong hydrogen bond interaction observed with Thr131 was also observed in H453361. It has been observed that the hydrogen bonds interacting with Thr131 have a positive effect on the bonding. When the hydrogen bond interactions of the compound coded J193055, which ranks third when the binding energies are compared, are examined, it can be expected that it will show better activity than the compounds coded I197821 and H453361. In line with these investigations, molecular dynamics simulation to the compound and studies are envisaged in the next step.

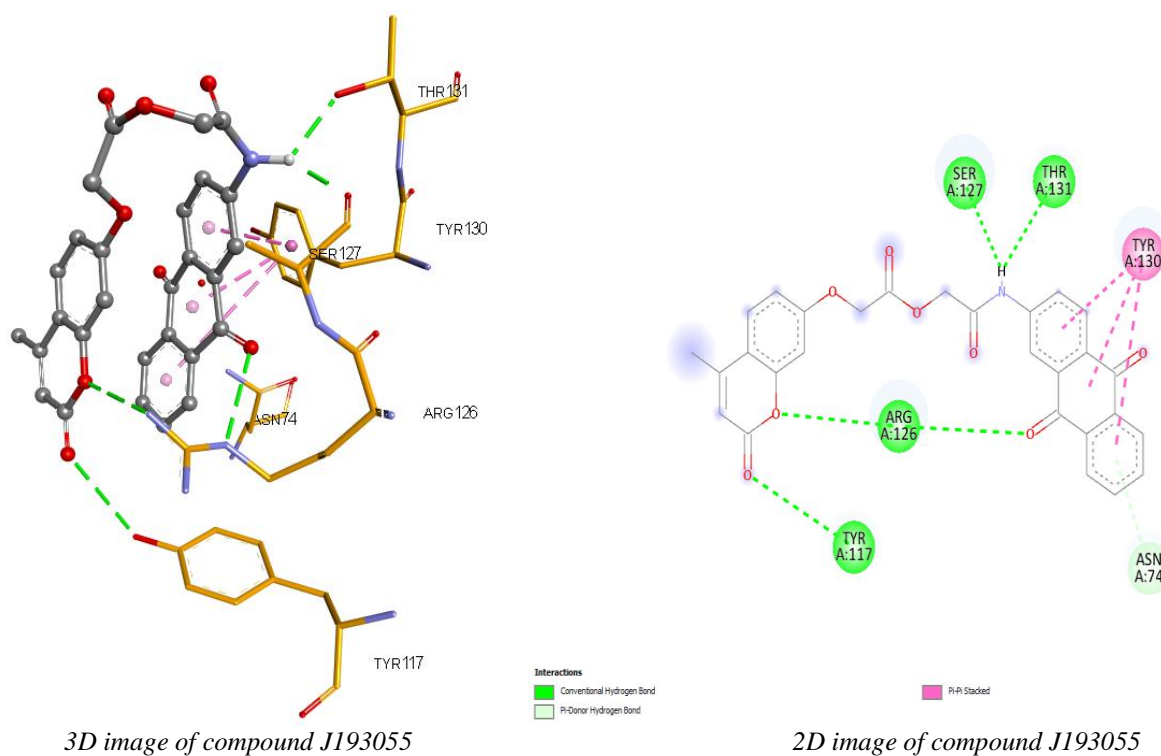


**Figure 3.4** 3D and 2D image of J193055 compound

Pi-pi stacking hydrophobic interaction was observed with Tyr130, which was seen similarly in the compounds with the codes I197821, H453361, and J193055, in the J193395 compound, in the 6PW compound (*as shown in Figure 3.5*). In addition to hydrophobic interactions, Thr131 pi-sigma interaction was also observed. There were strong hydrogen bonds observed in compound J193395 in addition to the reference compound 6PW. These are strong hydrogen bonds interacting with Ser127, and Thr131. Although these two hydrogen bonds have a high effect on strong bonding, the interactions are common with the compound coded J193055. In addition, the strong hydrogen bond interaction observed with Thr131 was also observed in H453361, and J193055 coded compounds. It was observed that the hydrogen bonds interacting with Thr131 had a positive effect on the interaction in all three compounds. When the hydrogen bond interactions of the compound coded J193395, which ranks fourth when the binding energies are compared, are examined, it can be expected that it will show a better activity than the compounds coded I197821 and H453361. In line with these investigations, applying molecular dynamics simulation and studies to this compound is envisaged in the next stage.

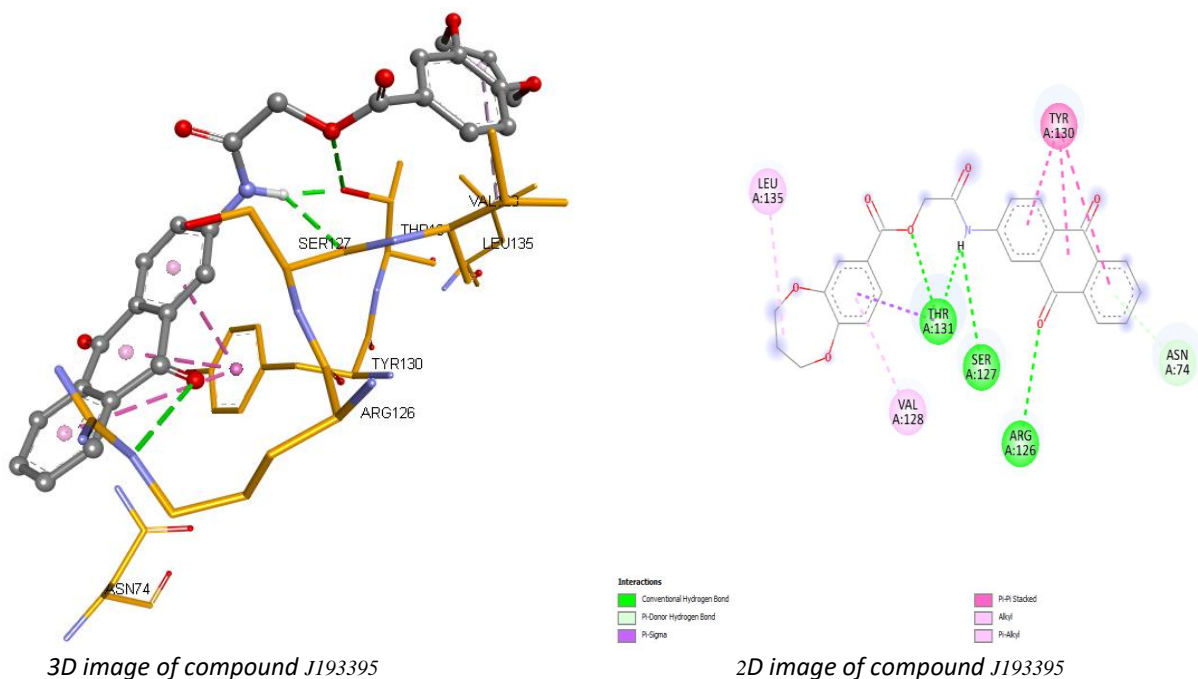


**Figure 3.5** 3D and 2D image of J193395 compound

2D and 3D images of the interaction of the H415814 with the mPGES-1 enzyme are given in **Figure 3.6** for comparison with others. Pi-pi stacking hydrophobic interaction was observed in H415814 with Tyr130, which was similarly seen in 6PW. Pi-cation hydrophobic interactions were also observed with Arg126, Arg70, and Arg73, which was not observed in 6PW. In addition to the reference compound 6PW, H415814 was observed to form strong hydrogen bonds with Arg126, Tyr117, and Arg73. Although the effect of these strong hydrogen bonds and hydrophobic interactions on strong bonds is positively reflected, it is not thought to provide better inhibition than the other four compounds.

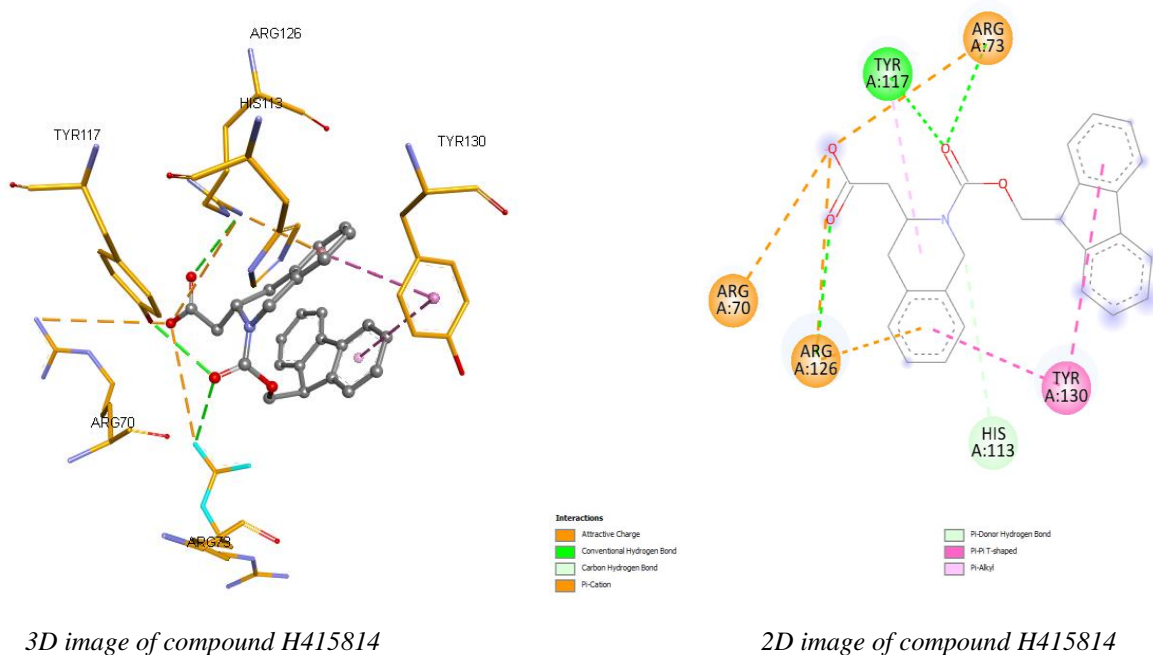


**Figure 3.6** 3D and 2D image of H415814 compound

In addition to the reference compound 6PW, H455638 was observed to form hydrogen bonds with Glu77. 2D and 3D images of the interaction of the H455638, with the mPGES-1 enzyme are given in Figure 3.7 for comparison with other. Pi-pi stacking hydrophobic interaction was observed in H455638 with Tyr130, which was similarly seen in 6PW. Pi-cation hydrophobic interactions with Arg73, which were not observed in 6PW, were also observed.

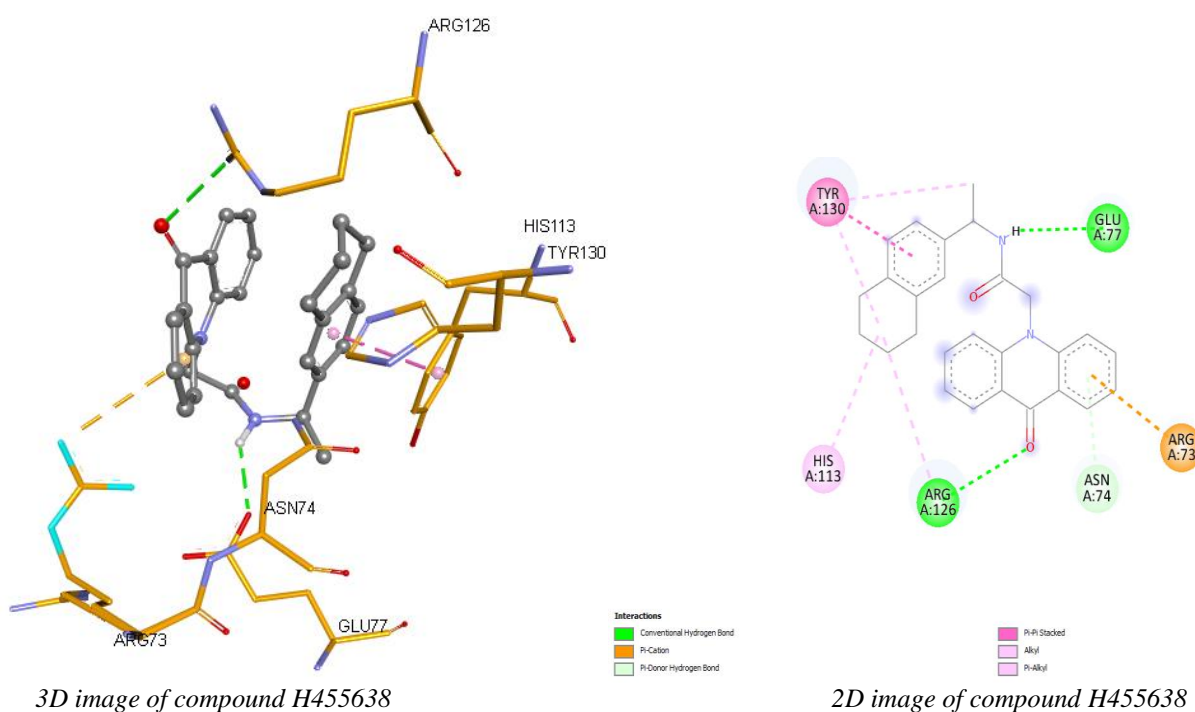


**Figure 3.7** 3D and 2D image of H455638 compound

2D and 3D images of the interaction of the I198359 with the mPGES-1 enzyme are given in **Figure 3.8** for comparison with others. Pi-pi stacking hydrophobic interaction was observed with Tyr130, similarly seen with compound I198359, compound 6PW, and other ligands. In addition to the reference compound 6PW, I198359 was observed to form hydrogen bonds with Arg73, Tyr117, and His113.

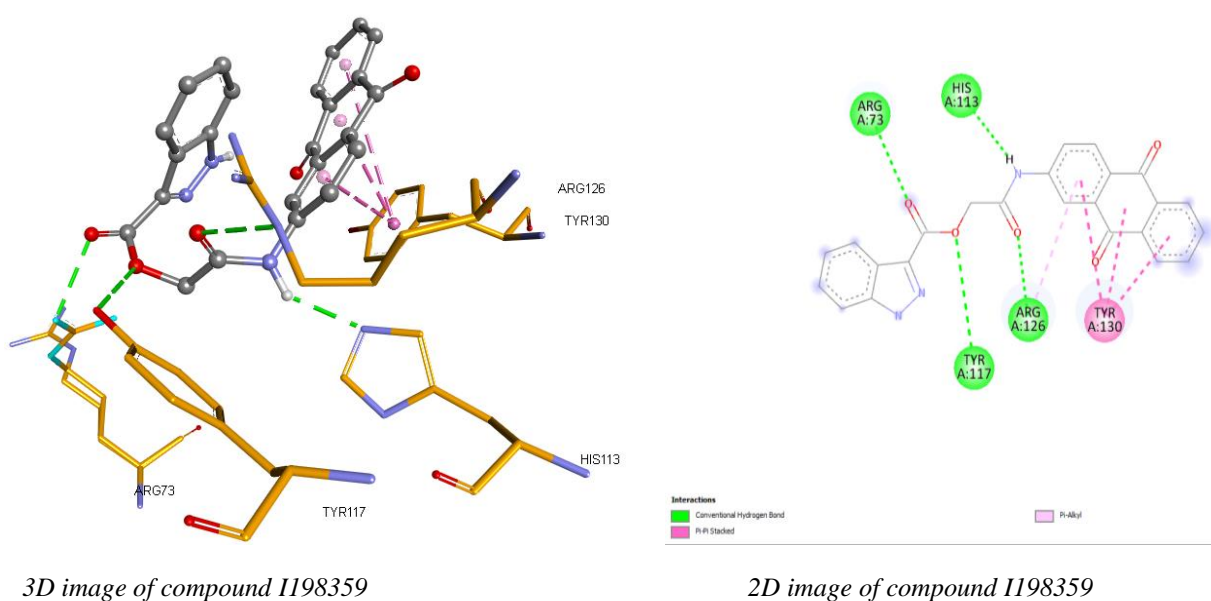


**Figure 3.8** 3D and 2D image of I198359 compound

2D and 3D images of the interaction of the I318035 with the mPGES-1 enzyme are given in **Figure 3.9** for comparison with others. Pi-pi stacking hydrophobic interaction with Tyr130 was observed in compound I318035, compound 6PW and similarly seen with other ligands. The hydrophobic interaction of Tyr130 with pi-sulfur, which was not observed in the reference compound and other compounds, was also observed in this compound. Although the pi-sulfur interaction was observed for the first time, no positive effect was observed. In addition to the reference compound 6PW, I318035 was observed to form hydrogen bond with Thr131.

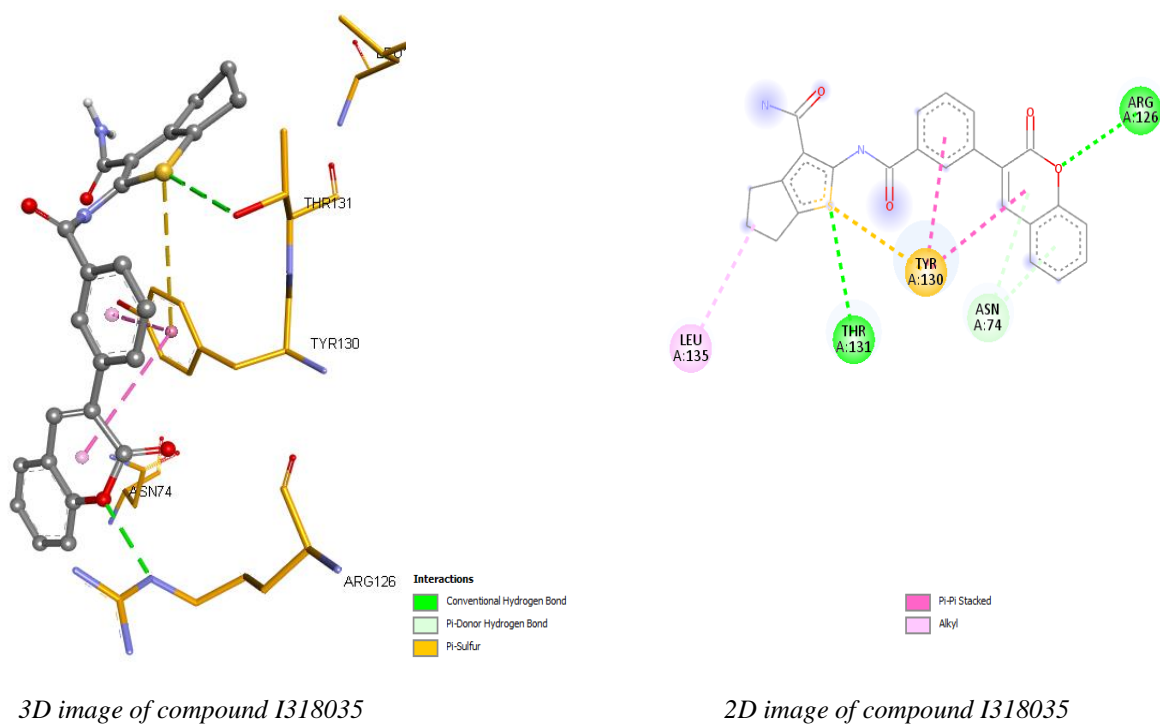
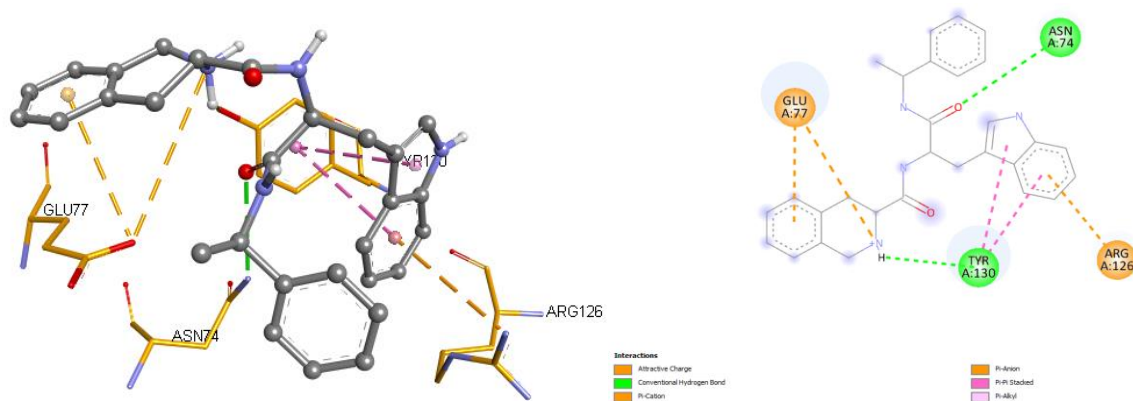


**Figure 3.9** 3D and 2D image of I318035 compound

In addition to the reference compound 6PW, J208987 was observed to form hydrogen bond with Tyr130. 2D and 3D images of the interaction of the J208987, with the mPGES-1 enzyme are given in **Figure 3.10** for comparison with other. Pi-pi stacking hydrophobic interaction was observed with Tyr130, similarly seen with J208987, 6PW, and other ligands. Pi-cation hydrophobic interactions with Arg126 and Glu77, which were not observed in the reference compound, were also observed in this compound.

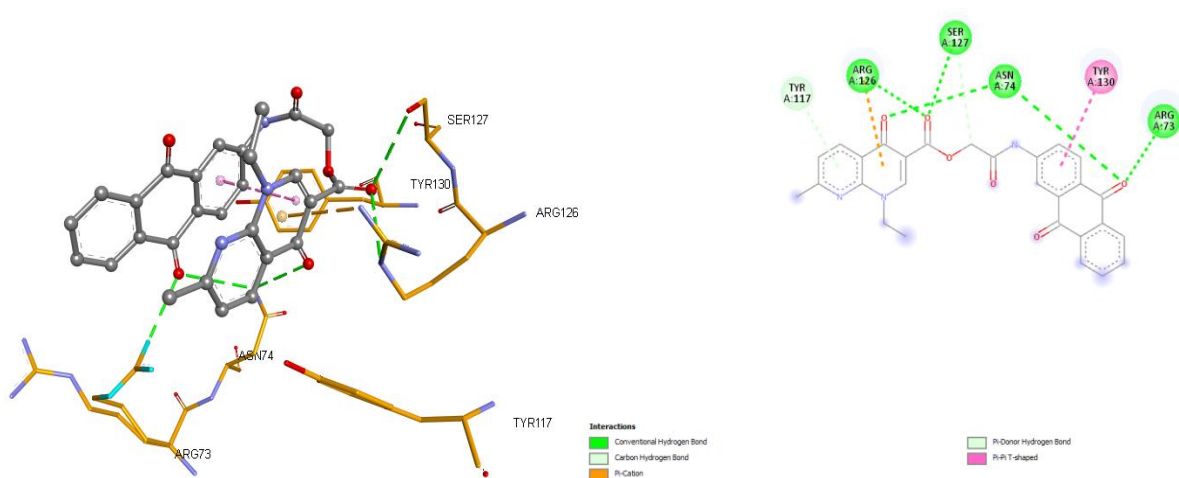


3D image of compound J208987

2D image of compound J208987

**Figure 3.10** 3D and 2D image of J208987 compound

Pi-pi stacking hydrophobic interaction was observed with Tyr130, similarly seen with J193203, compound 6PW, and other ligands (*as shown in Figure 3.11*). Pi-cation hydrophobic interaction with Arg126, which was observed in some other ligands but not in the reference compound, was also observed in this compound. In addition to the reference compound 6PW, I193203 was observed to form hydrogen bonds with Ser127, Asn74, and Arg73. Although many hydrogen bond interactions are seen in this compound, it is observed that the effect of these bonds on the bonding is low. The reason for this is thought to be only hydrogen bonds with oxygen.



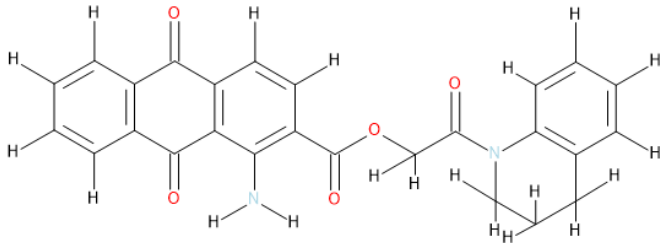
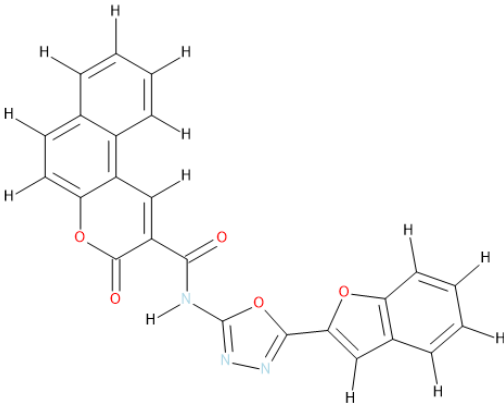
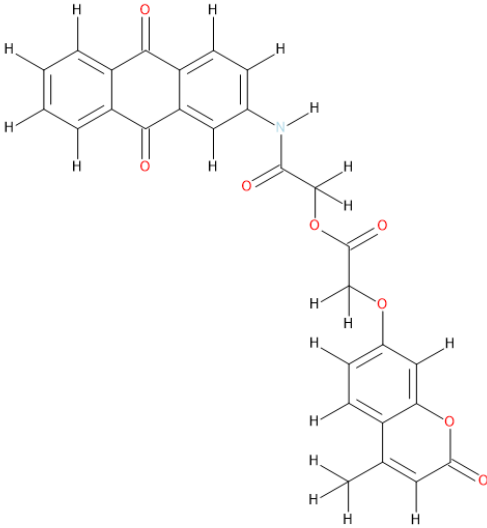
3D image of compound J193203

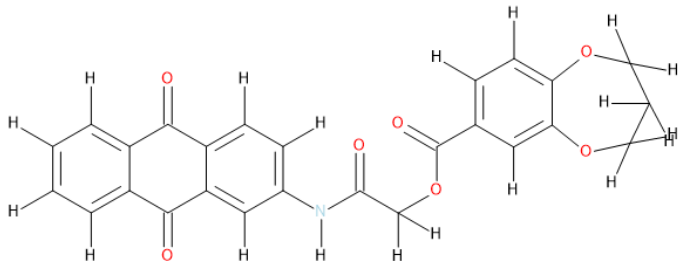
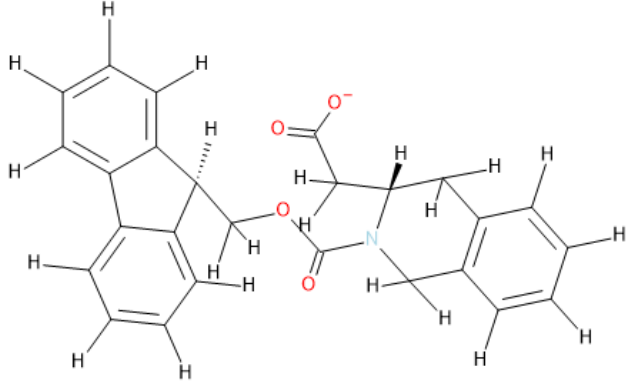
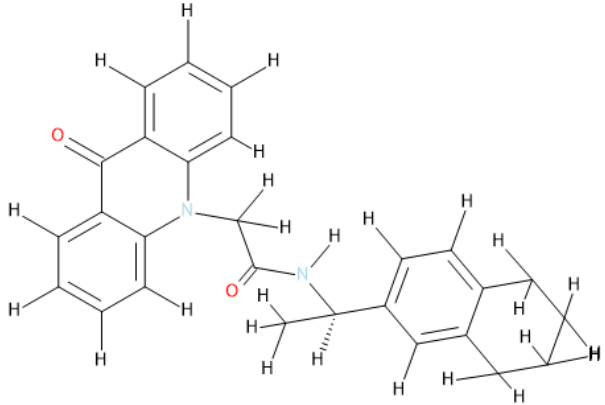
2D image of compound J193203

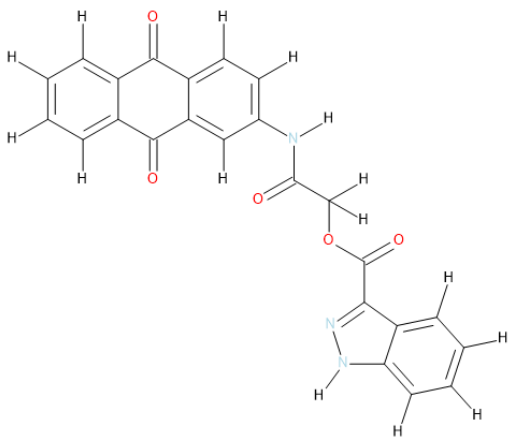
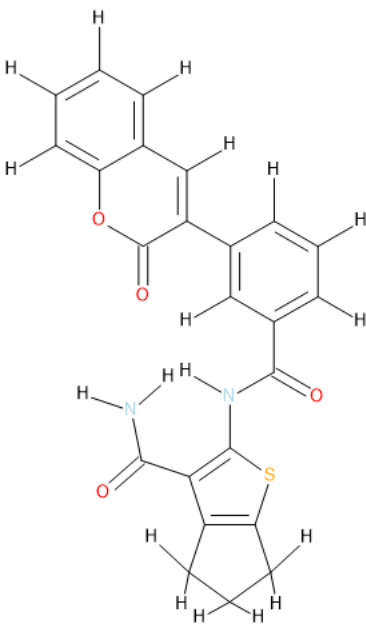
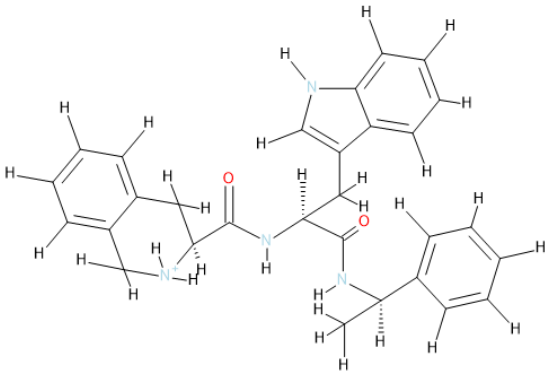
**Figure 3.11** 3D and 2D image of J193203 compound

As a result of the interactions of the ligands with the mPGES-1 enzyme in *Table 3.3*, the joint binding interactions of the ligands with the enzyme were observed. These ligand's 2D structures are shown in *Figure 3.12*. The pi-pi stacking interaction with Tyr130 has been observed in almost all ligands. Therefore, it is thought that the effect of Tyr130 and pi-pi stacking interaction on binding is very high. Although the variety of hydrogen bonds made varies, which region of the ligand the protein interacts with is considered an important factor.



Compound 2D Structure	Compound ID
 <p>The structure of compound I197821 consists of a central pyridine ring substituted with two benzene rings and a methylamino group. One of the benzene rings is further substituted with a methylamino group, which is connected via a methylene bridge to another methylamino group, which is in turn connected to a second benzene ring.</p>	<p><b>I197821</b></p>
 <p>The structure of compound H453361 features a central pyridine ring substituted with two benzene rings and a methylamino group. One of the benzene rings is substituted with a methylamino group, which is connected to a benzimidazole ring system, which is further substituted with another benzene ring.</p>	<p><b>H453361</b></p>
 <p>The structure of compound J193055 consists of a central pyridine ring substituted with two benzene rings and a methylamino group. One of the benzene rings is substituted with a methylamino group, which is connected to a methylamino group, which is in turn connected to a benzene ring substituted with a methylamino group.</p>	<p><b>J193055</b></p>

	<b>J193395</b>
	<b>H415814</b>
	<b>H455638</b>

	<b>I198359</b>
	<b>I318035</b>
	<b>J208987</b>

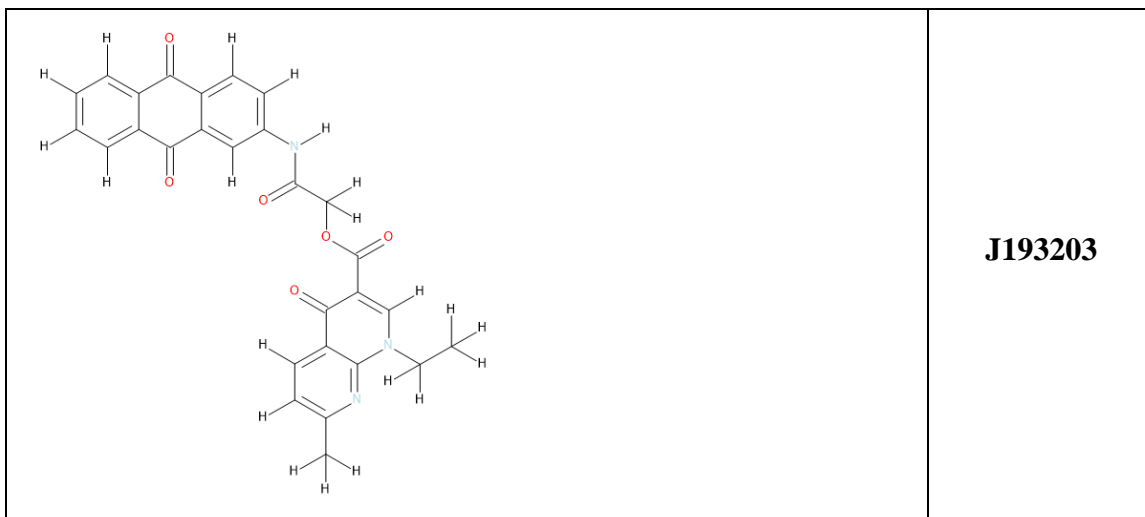


**Figure 3.12** 2D Molecule structures of highly potent ligands

### 3.3 ADMET Results

The predicted drug-like and ADMET properties of 10 potentially potent inhibitors of mPGES-1 were investigated. SMILES codes of compounds were generated from constructs using Biovia Discovery Studio 4.5 (DS) (Dassault Systemes BIOVIA, 2017) molecular editor software.

ADME properties are performed for LogP, LogS, hydrogen bond acceptor (nON) and donor (nOHN), rotatable bond number (nRot), topological polar surface area (TPSA), absorption (%ABS), and simple molecular identifiers. Lipinski "rule of five" and Veber are given as shown in **Table 3.4**.

LogP is a vital value indicating lipophilicity, and according to Lipinski's five rule, the logP value should be  $\leq 5$  (Lipinski, 2004). LogP value was found to be less than 5 for all compounds screened. LogS is the aqueous solubility predicted from the molecular structure, and all molecules were found to be moderately soluble.

The number of hydrogen bond donors ranges from 0 to 4, and the number of hydrogen bond acceptors ranges from 2 to 8. According to Lipinski's rule of five, these values must

be less than 5 and 10, respectively. None of the compounds violated this Lipinski rule. All tested compounds have less than ten rotatable bonds, indicating low conformational flexibility.

Total polar surface area (TPSA) is an essential property of a molecule in its transport across biological membranes. High TPSA values lead to poor bioavailability and absorption of a drug. The calculated absorption percentages for the ten compounds studied ranged from 51% to 130%. Any compound that violates more than 1 of these properties is likely to have poor absorption and oral bioavailability (Lipinski, 2004).

<b>Compound Code</b>	<b>MW (g/mol)</b>	<b>HBA</b>	<b>HBD</b>	<b>nRot Bond</b>	<b>Log Po/w</b>	<b>LogS (ESOL)</b>	<b>TPSA (Å<sup>2</sup>)</b>	<b>Lipinski Rule</b>	<b>Veber's Rule</b>
<b>I197821</b>	440,45	5	1	5	3,09	-5,21	106,77	Yes	Yes
<b>H453361</b>	423,38	7	1	4	3,78	-5,66	111,37	Yes	Yes
<b>J193055</b>	497,45	8	1	8	3,29	-5,09	128,98	Yes	Yes
<b>J193395</b>	457,43	7	1	6	3,20	-5,00	108,00	Yes	Yes
<b>H415814</b>	412,46	4	0	6	3,70	-5,16	69,67	Yes	Yes
<b>H455638</b>	410,51	2	1	5	4,49	-6,14	51,10	Yes	Yes
<b>I198359</b>	425,39	6	2	6	2,86	-4,83	118,22	Yes	Yes
<b>I318035</b>	430,48	4	2	5	4,06	-5,52	130,64	Yes	Yes
<b>J208987</b>	467,58	2	4	9	2,55	-5,15	90,60	Yes	Yes
<b>J193203</b>	495,48	7	1	7	3,05	-4,82	124,43	Yes	Yes

MW: Molecular weight; HBA: Number of hydrogen acceptors; HBD: Number of hydrogen donors; nRot: Number of rotatable bonds; LogP o/w: Consensus; LogS (ESOL): Estimating aqueous solubility from molecular structure; TPSA: Topological polar surface area.

**Table 3.4** Solubility and molecular descriptors of best ten compounds from SwissADME.

Caco-2 permeability is used to predict human intestinal permeability by measuring the

rate of drug molecule transport across the Caco-2 cell line (Van Breemen & Li, 2005). It was observed that the Caco-2 permeability was following the normal range of the drug molecule and the 10 drug precursor compounds tested showed high Caco-2 permeability.

P-glycoprotein (P-gp) is an ATP-dependent transmembrane protein and plays an essential role in drug absorption and penetration through the blood-brain barrier (BBB). This protein can be found in excess in tumor cells and leads to drug resistance (De Klerk et al., 2009). Except for compound H455638 of the selected compounds, none of the nine prodrug compounds were substrates for P-gp. In addition, eight precursor compounds, except H455638 and H415814, had no BBB permeability.

Although ten active precursor compounds were considered safe based on in silico toxicity studies for AMES toxicity, mutagenicity, tumorigenicity, and reproductive effects, these active compounds were observed to have toxic potential.

PAINS (Baell & Holloway, 2010) and Brenk (Brenk et al., 2008) stimulus data are known to recognize the part in a molecule that may cause some undesirable effects in vivo. PAINS and Brenk values and drug similarity values for selected active compounds are given in *Table 3.5*.

**Table 3.5** Predicted ADMET properties and drug-likeness of best ten compounds.

Compound Code	I197821	H453361	J193055	J193395	H415814	H455638	I198359	I318035	J208987	J193203
<b>ADMET Properties</b>										
Caco2 permeability (10-6cm/s) <sup>4</sup>	High	High	High	High	High	High	High	High	High	High
% Human intestinal absorption <sup>4</sup>	High	High	High	High	High	High	High	High	Low	High
P-glycoprotein substrates <sup>2</sup>	No	No	No	No	No	Yes	No	No	Yes	No
BBB permeations <sup>2</sup>	No	No	No	No	Yes	Yes	No	No	No	No
CNS permeability <sup>1</sup>	Yes	Yes	Yes	Yes	No	No	Yes	Yes	Yes	Yes
CYP1A2 inhibitors <sup>2</sup>	No	No	No	No	No	Yes	Yes	No	No	No
CYP2C19 inhibitors <sup>2</sup>	Yes	No	Yes	Yes	Yes	Yes	Yes	Yes	Yes	Yes
CYP2C9 inhibitors <sup>2</sup>	Yes	No	Yes	Yes	Yes	Yes	Yes	Yes	Yes	Yes
CYP2D6 inhibitors <sup>2</sup>	No	No	No	No	Yes	No	No	No	No	No
CYP3A4 inhibitors <sup>2</sup>	Yes	No	Yes	Yes	Yes	Yes	No	Yes	Yes	Yes
Total Clearance (log ml/min/kg)	-0,019	0,514	0,582	0,212	0,564	1,043	0,233	-0,402	1,402	0,529
AMES toxicity <sup>1</sup>	Yes	No	No	No	No	Yes	No	No	No	No
Mutagenic <sup>3</sup>	High	High	Low	Low	High	None	Low	None	None	Low
Tumorigenic <sup>3</sup>	High	High	High	High	High	None	High	None	None	High
Reproductive <sup>3</sup>	None	None	High	None	None	None	High	High	None	None
Irritant <sup>3</sup>	High	None	High	High	None	None	High	None	None	High
PAINS <sup>2</sup>	2 alerts	0 alert	1 alert	1 alert	0 alert	0 alert	1 alert	0 alert	0 alert	1 alert
Brenks <sup>2</sup>	1 alert	2 alerts	1 alert	0 alert	0 alert	1 alert	0 alert	1 alert	0 alert	0 alert
Drug-likeness <sup>3</sup>	3.119	0.9826	-3.8991	1.8794	-1.874	-3.1325	4.0928	1.6376	5.044	1.8854

<sup>1</sup>These studies were performed by using online webserver pkCSM (<http://biosig.unimelb.edu.au/pkcsm>)

<sup>2</sup>These studies were performed by using online webserver SwissADME (<http://www.swissadme.ch>)

<sup>3</sup>These studies were performed by using OSIRIS data warrior software (<http://www.openmolecules.org/datawarrior>)

<sup>4</sup>These studies were performed by using online webserver AdmetSAR (<http://lmmd.ecust.edu.cn/admetSar2/>)

The BOILED-Egg prediction model is obtained by combining both ellipses. The physicochemical area of molecules most likely to be absorbed by the gastrointestinal tract is the white area. The physicochemical area of molecules most likely to penetrate the brain is the yellow zone. The yellow and white areas are the areas that support each other (Daina & Zoete, 2016). Nine of the ten compounds examined, except for I318035, remained inside the rings given in *Figure 3.13*.

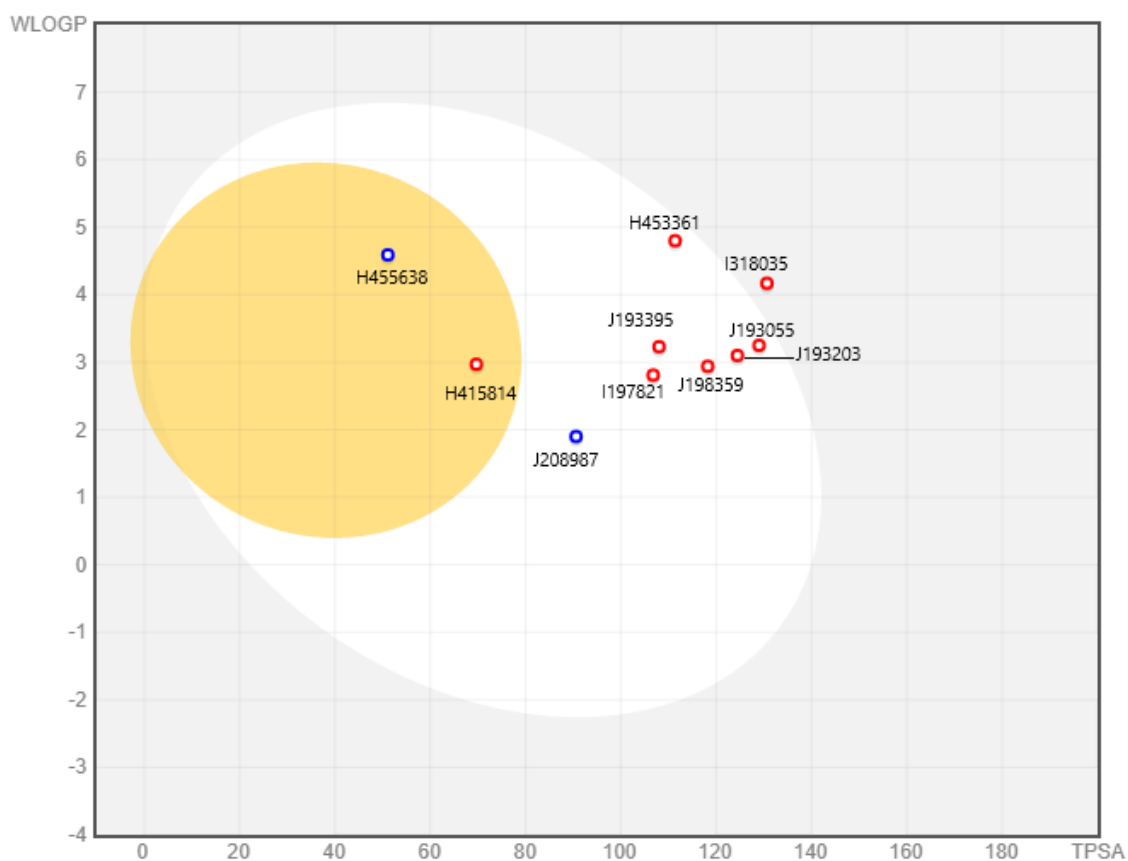


**Figure 3.13** The predictive model of BOILED-Egg for the best ten drug precursor molecules.



### 3.4 Molecular Dynamic Simulation Results

As a result of AutoDock-Vina, AutoDock 4 scanning, and ADMET examinations, five compounds (I197821, H453361, J193055, J193395 and 6PW(reference compound) that used for comparison) that were decided to perform MD simulations were simulated with 50 ns production. Root mean square deviation (RMSD), root mean square fluctuation (RMSF), radius of rotation (Rg) profiles of the four simulated systems were calculated to evaluate the stability of the complexes. All inhibitors remained bound to the enzyme throughout the MD simulation. It has been observed that all inhibitors that remain bound to the enzyme, which is responsible for inhibiting the activity of enzymes, retain their interactions.

#### 3.4.1 Root mean square deviation (RMSD)

The stability of each free isoform and its complex with its respective ligand was investigated by analyzing simulation parameters. RMSD can be used in drug design to measure the stability of a fixed protein-ligand complex. For mPGES-1, the backbone RMSD profiles of both free and complexes ranged from 1.5 to 4.5 Å (*Figure 3.14 (a), (b), (c), (d) and (e)*). Although the stability of the complexes changed until the end of the simulation, the complexes showed good stability close to the protein and similar to 6PW (reference compound) at the end of the simulation. In addition, the RMSD of the free form of mPGES-1 was synchronized with that of the complex between 40-50 ns. The RMSD of free and complex forms of mPGES-1 fluctuated up to 40 ns, with the complex tending to show lower stability than the free enzyme towards the end of the simulation (*Figure 3.14 (a) and (e)*). A similar trend was observed with the RMSD of free and complex forms of mPGES-1 up to 30 ns, although the bound form appeared to be more stable; as the simulation progressed, the complex showed lower stability than the free enzyme (*Figure 3.14 (c)*). Likewise, bound mPGES-1 showed lower RMSD than its free form during the simulation process (*Figure 3.14 (b) and (d)*). When the RMSD of free and bound forms were examined, some fluctuations were observed, and it was estimated

that loops in the protein's structure caused these fluctuations.

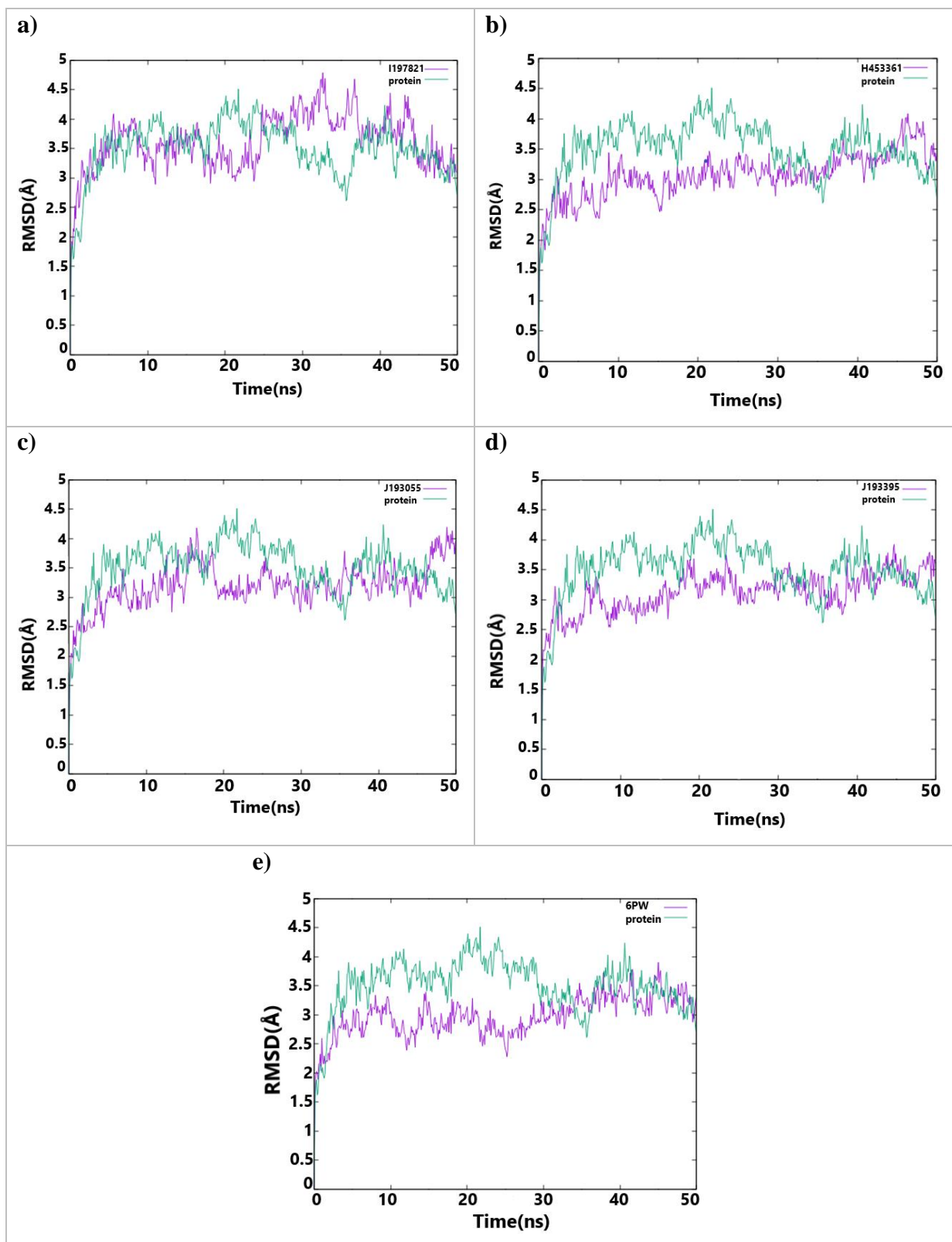


**Figure 3.14** 50 ns-MD simulation RMSD profiles of free mPGES-1 and bound mPGES-1 enzyme. mPGES-1 without ligand (green) and mPGES-1 with compounds complex (purple); the complex showed higher stability over simulation time. **(a).** mPGES-1 without ligand (green) and mPGES-1 compound I197821 (ZINC id; ZINC000008826383) complex (purple); towards the middle of the simulation period, the RMSD of the two systems was found to be simultaneous, with the complex showing equal stability with the free enzyme as the simulation progressed. **(b).** mPGES-1 without ligand (green) and mPGES-1 with compound H453361 (ZINC id; ZINC000009169466) complex (purple); although the RMSD of free and bound forms was found to be more stable between 35 and 40 ns as the simulation progressed, the complex showed higher stability than the free enzyme when looking at the beginning and end. **(c).** mPGES-1 without ligand (green) and mPGES-1 with compound J193055 (ZINC id; ZINC000009402864) complex (purple); although the two systems were found to be somewhat simultaneous until the end of the simulation, after 40 ns, the complex showed higher stability **(d).** mPGES-1 without ligand (green) and mPGES-1 with compound J193395 (ZINC id; ZINC000021416237) complex (purple); as in the image in c, although the two systems were found to be somewhat synchronized until the end of the simulation, the complex showed higher stability after 40 ns. **(e).** mPGES-1 without ligand (green) and mPGES-1 with compound 6PW complex (purple); an rmsd value similar to the picture in b,c,d was seen. The complex showed higher stability after 30 ns.

### 3.4.2 Root mean square fluctuation (RMSF)

The RMSF profile of the system shows the variation of residual fluctuation over time. Observation of fewer residues in the complexes showed increased RMSFs relative to the free isoforms. In other words, residues involved in interaction with inhibitors showed lower fluctuation, increasing the stability of the complexes (*Figure 3.15*)

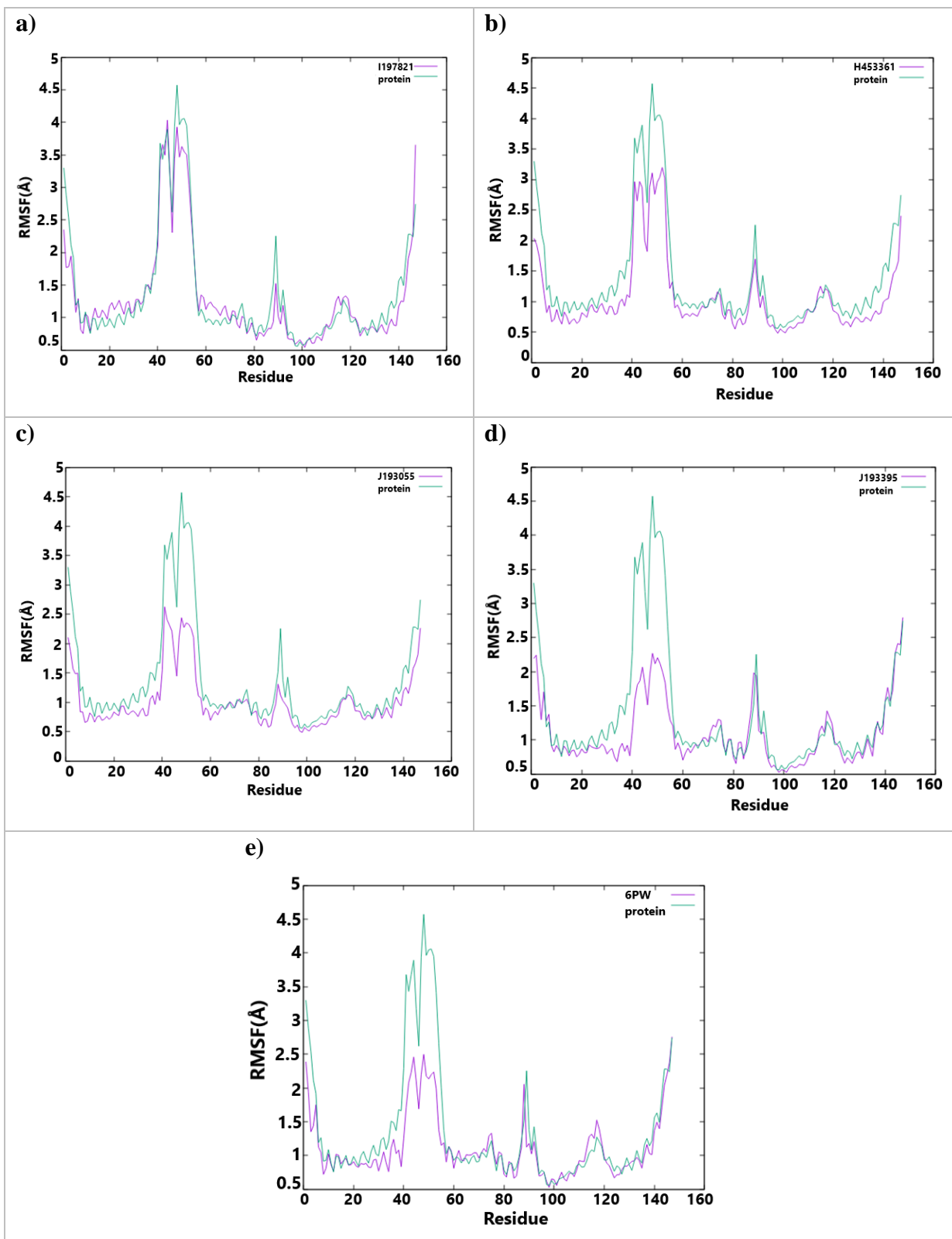


**Figure 3.15** RMSF profiles of the free mPGES-1 and bound mPGES-1 enzyme. mPGES-1 without ligand (green) and mPGES-1 with compounds complex (purple) **(a)**. mPGES-1 without ligand (green) and mPGES-1 compound I197821 (ZINC id; ZINC000008826383) complex (purple) **(b)**. mPGES-1 without ligand (green) and mPGES-1 with compound H453361 (ZINC id; ZINC000009169466) complex (purple) **(c)**. mPGES-1 without ligand (green) and mPGES-1 with compound J193055 (ZINC id; ZINC000009402864) complex (purple) **(d)**. mPGES-1 without ligand (green) and mPGES-1 with compound J193395 (ZINC id; ZINC000021416237) complex (purple) **(e)**. mPGES-1 without ligand (green) and mPGES-1 with compound 6PW complex (purple)

### **Radius of gyration (Rg)**

The radius of rotation (Rg) indicates the 3D structural stability and compactness of the protein structure. Here, the Rg profile of the complexes was found to range from 1.31-1.45 Å, while the free mPGES-1 ranged from 1.32 to 1.46 Å throughout the simulation. Thus, in the case of mPGES-1 complex assemblies, the Rg values were found to be consistent with the RMSD and RMSF distributions ( *Figure 3.16* ).

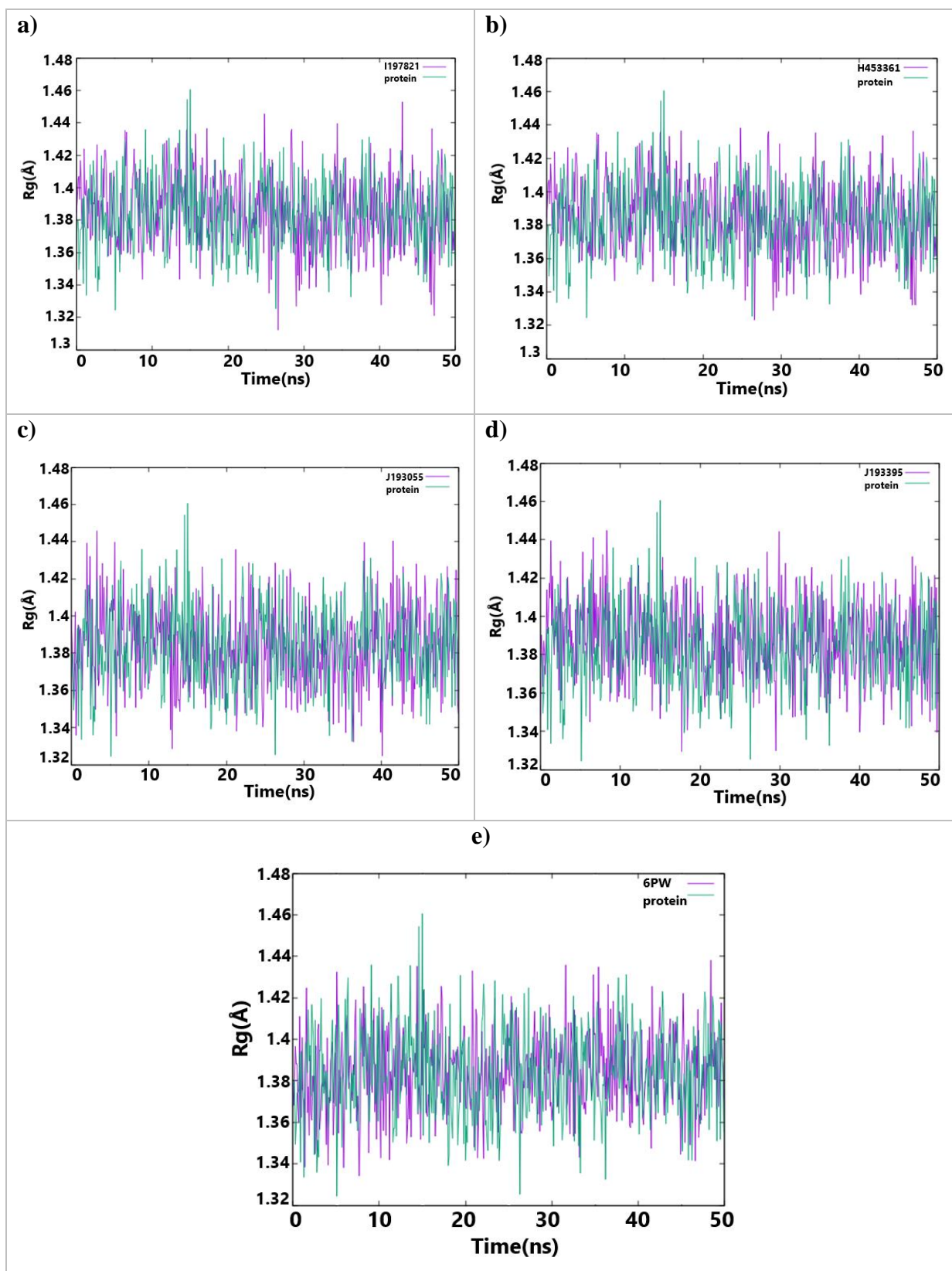


**Figure 3.16** Rg profiles of the free mPGES-1 and bound mPGES-1 enzyme. mPGES-1 without ligand (green) and mPGES-1 with compounds complex (purple) **(a)**. mPGES-1 without ligand (green) and mPGES-1 compound I197821 (ZINC id; ZINC000008826383) complex (purple) **(b)**. mPGES-1 without ligand (green) and mPGES-1 with compound H453361 (ZINC id; ZINC000009169466) complex (purple) **(c)**. mPGES-1 without ligand (green) and mPGES-1 with compound J193055 (ZINC id; ZINC000009402864) complex (purple) **(d)**. mPGES-1 without ligand (green) and mPGES-1 with compound J193395 (ZINC id; ZINC000021416237) complex (purple) **(e)**. mPGES-1 without ligand (green) and mPGES-1 with compound 6PW complex (purple). High fluctuating residues are indicated on the plots.

## 4.CONCLUSION

In this study, three new inhibitors (H453361, J193055, and J193395) were determined to be mPGES-1 potent inhibitors.

Reference compound 6PW is a selective potent inhibitor for mPGES-1. However, compared to selected compounds from the screened compounds showed better inhibition than 6PW. Therefore, the inhibition capacity and selectivity of the screened compounds were compared with the inhibition value and exposures of 6PW.

Compounds I197821, H453361, J193055, and J193395 showed much better inhibition than known inhibitor that is 6PW, and other candidate ligands. Despite its good inhibition value, compound I197821 is not recommended due to its bonds and fluctuating RMSD value in MD Simulation.

All compounds under development by the in silico method in our study show much better affinity for mPGES-1 than 6PW.

Detailed analysis of these four compounds' 2D and 3D interactions shows that almost all candidates with  $\pi$ - $\pi$  interactions with Tyr130 and hydrogen bonding with Arg126 show much better inhibition.

According to the results of molecular simulation, root mean square deviation (RMSD), root mean square fluctuation (RMSF), radius of rotation (Rg) profiles of four simulated systems were calculated to evaluate the stability of the complexes. According to all these results, it was supported that the compounds are good inhibitors for mPGES-1. H453361, J193055 and J193395 compounds are thought to be very specific inhibitors because their RMSD values are more stable than expected. Especially when we look at the RMSD results (Figure 3.14), although the fluctuation of compound I197821 during the simulation is normal due to the looped structure of the protein, it is not recommended because these fluctuations are not observed in H453361, J193055 and J193395 compounds.

These compounds, which we can identify as mPGES-1 inhibitors, showed very reasonable ADMET properties (Figure 4.24). Not all ligands that pass ADMET are considered too high for blood-brain barrier penetration. Regarding in silico ADMET and drug similarity studies, all seven compounds, except H415814, H455638, and J208987, of all active compounds predicted to show high Caco-2 permeability and human intestinal absorption, are not substrates of P-gp. Lipinski and Veber's rules were no violations for the best active compounds with and without BBB and CNS permeability. Finally, based on in silico toxicity studies, the active compounds were found to have some toxic effects.

Consequently, using computational modeling and screening methods are invaluable tools for searching for suitable compounds. Furthermore, this procedure provides a process that saves a large amount of money and significantly shortens time.



We believe that the model compounds we developed in this study are H453361, J193055, and J193395; need validation in future wet-lab studies.

## REFERENCES

- Akasaka, H., So, S. P., & Ruan, K. H. (2015). Relationship of the Topological Distances and Activities between mPGES-1 and COX-2 versus COX-1: Implications of the Different Post-Translational Endoplasmic Reticulum Organizations of COX-1 and COX-2. *Biochemistry*, 54(23), 3707–3715. <https://doi.org/10.1021/acs.biochem.5b00339>
- Allouche, A. (2012). Software News and Updates Gabedit — A Graphical User Interface for Computational Chemistry Softwares. *Journal of Computational Chemistry*, 32, 174–182. <https://doi.org/10.1002/jcc>
- Amano, H., Hayashi, I., Endo, H., Kitasato, H., Yamashina, S., Maruyama, T., Kobayashi, M., Satoh, K., Narita, M., Sugimoto, Y., Murata, T., Yoshimura, H., Narumiya, S., & Majima, M. (2003). Host prostaglandin E2-EP3 signaling regulates tumor-associated angiogenesis and tumor growth. *Journal of Experimental Medicine*, 197(2), 221–232. <https://doi.org/10.1084/jem.20021408>
- Baell, J. B., & Holloway, G. A. (2010). New substructure filters for removal of pan assay interference compounds (PAINS) from screening libraries and for their exclusion in bioassays. *Journal of Medicinal Chemistry*, 53(7), 2719–2740. <https://doi.org/10.1021/jm901137j>
- Brenk, R., Schipani, A., James, D., Krasowski, A., Gilbert, I. H., Frearson, J., & Wyatt, P. G. (2008). Lessons learnt from assembling screening libraries for drug discovery for neglected diseases. *ChemMedChem*, 3(3), 435–444. <https://doi.org/10.1002/cmdc.200700139>
- Chang, H. H., & Meuillet, E. J. (2011). Identification and development of mPGES-1 inhibitors: Where we are at? *Future Medicinal Chemistry*, 3(15), 1909–1934. <https://doi.org/10.4155/fmc.11.136>
- Cheng, F., Li, W., Zhou, Y., Shen, J., Wu, Z., Liu, G., Lee, P. W., & Tang, Y. (2012). AdmetSAR: A comprehensive source and free tool for assessment of chemical ADMET properties. *Journal of Chemical Information and Modeling*, 52(11), 3099–3105. <https://doi.org/10.1021/ci300367a>
- D Isaacson, J L Mueller, J. C. N. and S. S. (2006). 基因的改变 NIH Public Access. *Bone*, 23(1), 1–7. <https://doi.org/10.1007/978-3-642-30331-9>
- Daina, A., Michielin, O., & Zoete, V. (2017). SwissADME: A free web tool to evaluate pharmacokinetics, drug-likeness and medicinal chemistry friendliness of small molecules. *Scientific Reports*, 7(March), 1–13. <https://doi.org/10.1038/srep42717>

- Daina, A., & Zoete, V. (2016). A BOILED-Egg To Predict Gastrointestinal Absorption and Brain Penetration of Small Molecules. *ChemMedChem*, 1117–1121. <https://doi.org/10.1002/cmdc.201600182>
- De Klerk, O. L., Willemsen, A. T. M., Roosink, M., Bartels, A. L., Harry Hendrikse, N., Bosker, F. J., & Den Boer, J. A. (2009). Locally increased P-glycoprotein function in major depression: A PET study with [<sup>11</sup>C]verapamil as a probe for P-glycoprotein function in the bloodbrain barrier. *International Journal of Neuropsychopharmacology*, 12(7), 895–904. <https://doi.org/10.1017/S1461145709009894>
- Ding, K., Zhou, Z., Hou, S., Yuan, Y., Zhou, S., Zheng, X., Chen, J., Loftin, C., Zheng, F., & Zhan, C. G. (2018). Structure-based discovery of mPGES-1 inhibitors suitable for preclinical testing in wild-type mice as a new generation of anti-inflammatory drugs. *Scientific Reports*, 8(1), 1–9. <https://doi.org/10.1038/s41598-018-23482-4>
- Finetti, F., Terzuoli, E., Bocci, E., Coletta, I., Polenzani, L., Mangano, G., Alisi, M. A., Cazzolla, N., Giachetti, A., Ziche, M., & Donnini, S. (2012). Pharmacological inhibition of microsomal prostaglandin E synthase-1 suppresses epidermal growth factor receptor-mediated tumor growth and angiogenesis. *PLoS ONE*, 7(7). <https://doi.org/10.1371/journal.pone.0040576>
- Foley, J. P. (1991). Resolution equations for column chromatography. *The Analyst*, 116(12), 1275–1279. <https://doi.org/10.1039/AN9911601275>
- Hamza, A., Zhao, X., Tong, M., Tai, H. H., & Zhan, C. G. (2011). Novel human mPGES-1 inhibitors identified through structure-based virtual screening. *Bioorganic and Medicinal Chemistry*, 19(20), 6077–6086. <https://doi.org/10.1016/j.bmc.2011.08.040>
- Hanaka, H., Pawelzik, S. C., Johnsen, J. I., Rakonjac, M., Terawaki, K., Rasmuson, A., Sveinbjörnsson, B., Schumacher, M. C., Hamberg, M., Samuelsson, B., Jakobsson, P. J., Kogner, P., & Rådmark, O. (2009). Microsomal prostaglandin E synthase 1 determines tumor growth in vivo of prostate and lung cancer cells. *Proceedings of the National Academy of Sciences of the United States of America*, 106(44), 18757–18762. <https://doi.org/10.1073/pnas.0910218106>
- Howe, L. R., Subbaramaiah, K., Kent, C. V., Zhou, X. K., Chang, S. H., Hla, T., Jakobsson, P. J., Hudis, C. A., & Dannenberg, A. J. (2013). Genetic deletion of microsomal prostaglandin e synthase-1 suppresses mouse mammary tumor growth and angiogenesis. *Prostaglandins and Other Lipid Mediators*, 106, 99–105. <https://doi.org/10.1016/j.prostaglandins.2013.04.002>
- Irwin, J. J., & Shoichet, B. K. (2005). for Virtual Screening. *Journal of Chemical Information and Modeling*, 45(1), 177–182.

- Jakobsson, P. J., Thorén, S., Morgenstern, R., & Samuelsson, B. (1999). Identification of human prostaglandin E synthase: A microsomal, glutathione-dependent, inducible enzyme, constituting a potential novel drug target. *Proceedings of the National Academy of Sciences of the United States of America*, *96*(13), 7220–7225. <https://doi.org/10.1073/pnas.96.13.7220>
- Jin, Y., Regev, A., Kam, J., Phipps, K., Smith, C., Henck, J., Campanale, K., Hu, L., Hall, D. G., Yang, X. Y., Nakano, M., McNearney, T. A., Uetrecht, J., & Landschulz, W. (2018). Dose-dependent acute liver injury with hypersensitivity features in humans due to a novel microsomal prostaglandin E synthase 1 inhibitor. *British Journal of Clinical Pharmacology*, *84*(1), 179–188. <https://doi.org/10.1111/bcp.13423>
- Kamata, H., Hosono, K., Suzuki, T., Ogawa, Y., Kubo, H., Katoh, H., Ito, Y., Uematsu, S., Akira, S., Watanabe, M., & Majima, M. (2010). MPGES-1-expressing bone marrow-derived cells enhance tumor growth and angiogenesis in mice. *Biomedicine and Pharmacotherapy*, *64*(6), 409–416. <https://doi.org/10.1016/j.biopha.2010.01.017>
- Kock, A., Larsson, K., Bergqvist, F., Eissler, N., Elfman, L. H. M., Raouf, J., Korotkova, M., Johnsen, J. I., Jakobsson, P. J., & Kogner, P. (2018). Inhibition of Microsomal Prostaglandin E Synthase-1 in Cancer-Associated Fibroblasts Suppresses Neuroblastoma Tumor Growth. *EBioMedicine*, *32*, 84–92. <https://doi.org/10.1016/j.ebiom.2018.05.008>
- Kuklish, S. L., Antonysamy, S., Bhattachar, S. N., Chandrasekhar, S., Fisher, M. J., Fretland, A. J., Gooding, K., Harvey, A., Hughes, N. E., Luz, J. G., Manninen, P. R., McGee, J. E., Navarro, A., Norman, B. H., Partridge, K. M., Quimby, S. J., Schiffler, M. A., Sloan, A. V., Warshawsky, A. M., ... Yu, X. P. (2016). Characterization of 3,3-dimethyl substituted N-aryl piperidines as potent microsomal prostaglandin E synthase-1 inhibitors. *Bioorganic and Medicinal Chemistry Letters*, *26*(19), 4824–4828. <https://doi.org/10.1016/j.bmcl.2016.08.023>
- Lee, J., Cheng, X., Swails, J. M., Yeom, M. S., Eastman, P. K., Lemkul, J. A., Wei, S., Buckner, J., Jeong, J. C., Qi, Y., Jo, S., Pande, V. S., Case, D. A., Brooks, C. L., MacKerell, A. D., Klauda, J. B., & Im, W. (2016). CHARMM-GUI Input Generator for NAMD, GROMACS, AMBER, OpenMM, and CHARMM/OpenMM Simulations Using the CHARMM36 Additive Force Field. *Journal of Chemical Theory and Computation*, *12*(1), 405–413. <https://doi.org/10.1021/acs.jctc.5b00935>
- Lipinski, C. A. (2004). Lead- and drug-like compounds: The rule-of-five revolution. *Drug Discovery Today: Technologies*, *1*(4), 337–341. <https://doi.org/10.1016/j.ddtec.2004.11.007>
- Lomize, A. L., Pogozheva, I. D., Lomize, M. A., & Mosberg, H. I. (2006). Positioning

of proteins in membranes: A computational approach. *Protein Science*, 15(6), 1318–1333. <https://doi.org/10.1110/ps.062126106>

Luz, J. G., Antonysamy, S., Kuklish, S. L., Condon, B., Lee, M. R., Allison, D., Yu, X. P., Chandrasekhar, S., Backer, R., Zhang, A., Russell, M., Chang, S. S., Harvey, A., Sloan, A. V., & Fisher, M. J. (2015). Crystal Structures of mPGES-1 Inhibitor Complexes Form a Basis for the Rational Design of Potent Analgesic and Anti-Inflammatory Therapeutics. *Journal of Medicinal Chemistry*, 58(11), 4727–4737. <https://doi.org/10.1021/acs.jmedchem.5b00330>

Melville, J. L., & Hirst, J. D. (2007). TMACC: Interpretable correlation descriptors for quantitative structure-activity relationships. *Journal of Chemical Information and Modeling*, 47(2), 626–634. <https://doi.org/10.1021/ci6004178>

Morris, G. M., Goodsell, D. S., Halliday, R. S., Huey, R., Hart, W. E., Belew, R. K., & Olson, A. J. (1998). Automated docking using a Lamarckian genetic algorithm and an empirical binding free energy function. *Journal of Computational Chemistry*, 19(14), 1639–1662. [https://doi.org/10.1002/\(SICI\)1096-987X\(19981115\)19:14<1639::AID-JCC10>3.0.CO;2-B](https://doi.org/10.1002/(SICI)1096-987X(19981115)19:14<1639::AID-JCC10>3.0.CO;2-B)

Murakami, M. (2011). Lipid mediators in life science. *Experimental Animals*, 60(1), 7–20. <https://doi.org/10.1538/expanim.60.7>

Norel, X. (2007). Prostanoid receptors in the human vascular wall. *TheScientificWorldJournal*, 7, 1359–1374. <https://doi.org/10.1100/tsw.2007.184>

Patrick Walters, W., Stahl, M. T., & Murcko, M. A. (1998). Virtual screening - An overview. *Drug Discovery Today*, 3(4), 160–178. [https://doi.org/10.1016/s1359-6446\(97\)01163-x](https://doi.org/10.1016/s1359-6446(97)01163-x)

Phillips, J. C., Braun, R., Wang, W., Gumbart, J., Tajkhorshid, E., Villa, E., Chipot, C., Skeel, R. D., Kalé, L., & Schulten, K. (2005). Scalable molecular dynamics with NAMD. *Journal of Computational Chemistry*, 26(16), 1781–1802. <https://doi.org/10.1002/jcc.20289>

Pires, D. E. V., Blundell, T. L., & Ascher, D. B. (2015). pkCSM: Predicting small-molecule pharmacokinetic and toxicity properties using graph-based signatures. *Journal of Medicinal Chemistry*, 58(9), 4066–4072. <https://doi.org/10.1021/acs.jmedchem.5b00104>

Sander, T., Freyss, J., Von Korff, M., & Rufener, C. (2015). DataWarrior: An open-source program for chemistry aware data visualization and analysis. *Journal of Chemical Information and Modeling*, 55(2), 460–473. <https://doi.org/10.1021/ci500588j>

- Sasaki, Y., Nakatani, Y., & Hara, S. (2015). Role of microsomal prostaglandin E synthase-1 (mPGES-1)-derived prostaglandin E2 in colon carcinogenesis. *Prostaglandins and Other Lipid Mediators*, *121*, 42–45.  
<https://doi.org/10.1016/j.prostaglandins.2015.06.006>
- Serhan, M., Sprowls, M., Jackemeyer, D., Long, M., Perez, I. D., Maret, W., Tao, N., & Forzani, E. (2019). Total iron measurement in human serum with a smartphone. *AIChE Annual Meeting, Conference Proceedings, 2019-Novem*.  
<https://doi.org/10.1039/x0xx00000x>
- Van Breemen, R. B., & Li, Y. (2005). Caco-2 cell permeability assays to measure drug absorption. *Expert Opinion on Drug Metabolism and Toxicology*, *1*(2), 175–185.  
<https://doi.org/10.1517/17425255.1.2.175>
- Van Rees, B. P., Sivula, A., Thorén, S., Yokozaki, H., Jakobsson, P. J., Offerhaus, G. J. A., & Ristimäki, A. (2003). Expression of microsomal prostaglandin E synthase-1 in intestinal type gastric adenocarcinoma and in gastric cancer cell lines. *International Journal of Cancer*, *107*(4), 551–556.  
<https://doi.org/10.1002/ijc.11422>
- Yamada, Y., Gohda, S., Abe, K., Togo, T., Shimano, N., Sasaki, T., Tanaka, H., Ono, H., Ohba, T., Kubo, S., Ohkubo, T., & Sato, S. (2017). Carbon materials with controlled edge structures. *Carbon*, *122*(October 1995), 694–701.  
<https://doi.org/10.1016/j.carbon.2017.07.012>
- Zhou, Z., Yuan, Y., Zhou, S., Ding, K., Zheng, F., & Zhan, C. G. (2017). Selective inhibitors of human mPGES-1 from structure-based computational screening. *Bioorganic and Medicinal Chemistry Letters*, *27*(16), 3739–3743.  
<https://doi.org/10.1016/j.bmcl.2017.06.075>

# CURRICULUM VITAE

## EDUCATION

**2019-2021** MsC in Bioinformatics, Computational Biology Simulation Lab, Kadir Has University – Fatih/İSTANBUL Graduation Degree is 3.59/4

**2015-2019** Bachelor Degree in Molecular Biology and Genetics, Çanakkale 18 Mart University, Çanakkale/TURKEY Graduation Degree is 3.17/4

**2014-2015** English Preparatory Education in Çanakkale 18 Mart University, Çanakkale/TURKEY

**2010-2014** Hüseyin Yıldız Anatolian High School, Beylikdüzü/İstanbul

## RELEVANT EXPERIENCES AND TRAINING

2019 Teaching Assistant, Computational and Molecular Genetics Laboratory, Kadir Has University

2018(3 Months) Çanakkale 18 Mart University – Molecular Biology Laboratory Advisor: Assoc. Prof. Tuğba Tumer ( tumertb@gmail.com) Acquired skills: Western Blot, PCR, Real Time PCR,ELISA

2018(2 Months) Intern,TÜBİTAK MAM - Molecular Vaccine Laboratory

Acquired Skills: Western Blot, Real Time PCR, Protein Precipitation, ELISA, Immunfluorescence and Confocal Microscopy technics.

Applications

- Quantitation of protein by Lawry and Bradford methods
- SDS PAGE of simA-9 supernatant for TNF-  $\alpha$
- BCA Assay for simA-9 supernatant
- RNA isolation from bend-3 P-15 seeding

- cDNA synthesis of THP-1 cells
- RT-PCR for raw264.7, NRF-2:NOS/COX-2, beta-actin
- Collection/Precipitation of supernatant with TCA method
- Western Blot of COX-2 and AMPK proteins in simA-9 cell line
- ELISA Assay with THP-1 cell line
- Nitric Oxide and MTT Assays of raw264.7 cells treated with N and S series
- Protein Extraction with NEPER method
- Recombinant DNA technology

2017(2 Month) Intern, Medicinal Genetics, Molecular Genetic Laboratory

- DNA isolation from peripheral bloodstream (more than 1000 times)
- DNA isolation from the tissue (more than 1000 times)
- DNA measurement with spectrophotometer (more than 1000 times)
- Protein isolation from rat liver
- Agarose Gel Electrophoresis
- NGS, ARRAY

## **POSTERS**

- AllerGene project: Production of a Applicable Diagnostic Kit for Detecting Allergens Causing AllergicDiseases
- Measurement of Nuclear Factor-Kappa B Translocation on Lipopolysaccharide-Activated Human Dendritic Cells by Confocal Microscopy, Aline Blaecke, YvesDelneste, Nathalie Herbault, Pascale Jeannin, Jean-Yves Bonnefoy, Alain



Beck, and Jean-Pierre Aubry\* Presented by: Gamze Ciftci, Advisor: Tuğba Tümer

## **PROJECT**

Computer Aided Design, Synthesis, Apoptosis, Angiogenesis and Investigation of MPGES-1 Enzyme Inhibitor Effects of Heteroaryl Sulfonyl Acetamides and Their Analogues with Possible Anticancer Effect

AllerGene Project: Home Assay Allergy Diagnostic Kit Production. With this kit to be produced, people can recognize their allergens without the need for a specialist, and therefore they can improve the quality of life by being more careful.

AllerGene is also an entrepreneurship project that started last year in Çanakkale Teknopark. With this project, we participated 6 competition and in Innostation competition, our project won first place. And also we applied for a patent. Our goal in the near future (2020) is to establish a company to produce this kit.

## **EXAM INFORMATION**

ALES Academic Staff and Graduate Education Entrance Exam (80.49/100)

YÖKDİL Foreign Language Examination for Higher Education Institutions (67.5/100)

## **SEMINARS AND COURSES**

- International Istanbul Technical University Molecular Biology and Genetics Student Congress'17 October 6-8 th, 2017 - Certificate of attendance
- Gençomü Biology Congress- 1-2 March 2018 – Certificate of attendance
- Acugen Life Sciences Congress – 09 February 2019- Certificate of attendance
- Gencomü Biology Congress- 1-2 March 2019 – Certificate of attendance
- Gebze Technical University - G.E.N 3 – 23-24 March 2019 – Certificate of attendance

- GebzeTechnicalUniversity - Evolution Days – 26-27 October 2019 – Certificate of attendance

## **COMPETENCIES**

Computer Skills Microsoft Office Windows(XP,7, Linux(ubuntu)

Minitab17

VMD 1.9.3 (3D Protein Modelling) AutoDock

PyMol Mendeley Python